Master Thesis
TVVR 20/5003

Modelling of Water Exchange in Flommen Lagoon System in Skanör-Falsterbo, Sweden

Kenny Lay
Kristian Ångbäck

Division of Water Resources Engineering
Department of Building and Environmental Technology
Lund University

Modelling of Water Exchange in Flommen Lagoon System in Skanör-Falsterbo, Sweden

By:
Kenny Lay
Kristian Ångbäck

Master Thesis

Division of Water Resources Engineering
Department of Building & Environmental Technology
Lund University
Box 118
221 00 Lund, Sweden

Water Resources Engineering
TVVR-20/5003
ISSN 1101-9824

Lund 2020
www.tvrl.lth.se

Master Thesis
Division of Water Resources Engineering
Department of Building & Environmental Technology
Lund University

English title:	<Modelling of Water Exchange in Flommen Lagoon System in Skanör-Falsterbo, Sweden>
Author(s):	<Kenny Lay> <Kristian Ångbäck>
Supervisor:	<Magnus Larson>
Examiner:	<Hans Hanson>
Language	<English >
Year:	2020
Keywords:	<water exchange, sedimentation, flommen lagoon system, iph-eco, modelling>

Abstract

The Flommen Lagoon system is located in Skanör-Falsterbo, Sweden. It hosts a diverse and sensitive ecosystem. There have been concerns about the water quality in this lagoon due to impaired water exchange.

The objectives of this thesis is to determine the current state of the water exchange in the lagoon and investigate possible measures to improve it. These possible measures revolve around the construction of a new inlet, and the potential closing of the inlet Slusan. Flow velocities, especially those in the inlet Slusan, will also be briefly elaborated upon in an effort to gain a better understanding of the sedimentation issues. At present, the sedimentation at the inlet is alleviated by regular dredging.

To accomplish these objectives, a hydrodynamic model of the Flommen Lagoon system was created. The modelling software IPH-ECO was used to create the model. This model was used to calculate the flushing time in the lagoon as a measure of the water exchange. Spatially distributed residence time was also calculated and used as a measure to investigate the water quality in different parts of the lagoon.

Simulation results indicate a flushing time of 33 days in the current state of the lagoon with Slusan open. Should a new inlet be built to compliment Slusan, then a flushing time of 22 days is expected. But this likely comes at a cost of increased sedimentation issues due to lower flow velocities at Slusan. If instead this new inlet is built and Slusan closed, then a flushing time beyond 60 days can be anticipated. This measure would reduce the costs associated with dredging, but cause a decline in the water quality in the lagoon.

Acknowledgements

Our sincere gratitude goes to Almir Nunes de Brito Junior, a doctoral student at Division of Water Resources Engineering, Lund University. Without his vast expertise in programming and experience in using IPH-ECO, it would have been very difficult to adapt the software for the prevailing conditions in the Flommen Lagoon system.

During the course of this thesis, our supervisor, Prof. Magnus Larson provided us with extraordinary guidance. We would like to extend our deepest appreciation to him.

Half a dozen field expeditions were conducted at the Flommen Lagoon system. We thank Clemens Klante for helping us measure bathymetry during one of the expeditions. We also extend our gratitude to Björn Almström for providing us with some of the equipment needed for the expeditions.

Our appreciation goes to Sebastian Bokhari Irminger, who gave us the source material needed to create a working model of Flommen Lagoon, and invited us to visit Sweco's office in Malmö, Sweden, to discuss the project.

This master thesis was mostly worked upon and completed within the comfy office room 1487 at the V-building, Lund University. Spanning the period of September 2019 - March 2020, this process has been a marvellous learning experience. Our colleagues that we shared this office with helped to brighten our days during the dark winter months.

Last but not least, we thank our friends and families for supporting us all along the way.

Glossary

Bathymetry: Underwater equivalent to topography.

Cartesian coordinate system: Coordinate system with that specifies each point using the distance from two perpendicular lines as reference.

Chézy coefficient: Friction coefficient describing energy loss.

Coriolis effect: Inertial force caused by the Earth's rotation around its axis.

DEM: Digital Elevation Model. A map containing topographic data.

Eddy viscocity: Coefficent connecting the average shear stress within a turbulent flow of water to the vertical gradient of velocity.

FLS: Flommen Lagoon System.

Fortran: Programming language that can be used for numerical computing.

GIS: Geographic Information System, is a system used to manage and analyse spatial or geographic data.

GUI: Graphical User Interface.

Holoscene: Geological epoch that began roughly 11650 years before present.

Hydrodynamic boundary condition: Start up conditions concerning the boundary and input data of the model.

Manning coefficient: Coefficient describing the roughness or friction applied to the water.

MATLAB: Software and programming language that can be used for numerical computing.

Morphology: Study concerning the shape and evolution of topography and bathymetry.

Contents

1 Introduction

1.1 Background

Coastal lagoons occur in the transitional zone between sea and land, constituting water bodies that are connected to the sea by one or several channels known as inlets. According to Barnes (1980), coastal lagoons occupy 13 percent of the total coastlines around the world. The water quality in a coastal lagoon is affected by the water exchange with the sea, e.g. the amount of water coming into the lagoon and the amount of water flowing out over a fixed period of time. The water exchange depends on several factors, such as wind, tides, waves, evaporation, and river flows. Should the water exchange not be sufficient, the resulting poor water quality might have a negative impact on the aquatic life. In many places the inlet is affected by sediment transport, leading to sedimentation, which can affect the water exchange capacity of the inlet. One possible way to alleviate this is to maintain the inlet channel through dredging or by constructing additional channels between the lagoon and the sea.

The coastal area around the Skanör-Falsterbo Peninsula, located in southern Sweden, is characterized by a complex coastal lagoon system. This system is located in the nature preserve of Flommen, with the inlet on its western side named Slusan. At normal sea water levels, the system consists of a number of separate water bodies that are connected through small channels. However, at high water levels in the sea, some water bodies merge and form a more coherent lagoon system, making it a challenge to estimate the flow in the system and its water exchange with the sea through Slusan. This exchange determines the water quality in the Flommen Lagoon system (FLS), and the conditions for aquatic life. In addition, flooding is a problem in the lagoon at extreme sea levels, although after the construction of retractable sluice gates to prevent flooding during coastal storms, this problem has partly been alleviated. These gates however, comes with a few issues. One concerns the gates themselves, as they could restrict the water exchange in Flommen even when the gates are not deployed. Another concern could be the gates aggravating the sedimentation found at Slusan.

1.2 Objectives

The first objective is to determine the water exchange in the FLS, including the details of the flow in various parts of the system. System-wide as well as local estimates of the residence time will be obtained in order to identify parts of the system where problems may potentially develop regarding water quality. The second objective is to investigate different measures that could enhance water exchange with the sea and thus improve water quality in the lagoon system. These measures revolve around constructing a new canal on the northern part of the lagoon, and possibly shutting down Slusan. The velocity through the inlet will also be investigated to evaluate the possible impact on inlet sedimentation.

1.3 Procedure

In September 2019, preparations for this thesis began with formulation of the project plan that revolved around the creation of a water exchange model of the FLS.

During the start-up phase of this thesis, a comprehensive literature study was carried out on coastal lagoons and related processes. Emphasis was put on the essence of water exchange, water balance and littoral sediment transport. A literature study regarding the FLS was also conducted with focus on climatology, geology and local coastal processes in the area. However, previous literature about the lagoon itself were scarce.

Existing background data of the area was gathered. This includes water level data from a measuring station in Skanör Harbour, near the inlet of the lagoon. Wind data and topographic data was also obtained. These data sets were vital for the process of generating a hydrodynamic model of the FLS. Water level data from the harbour along with wind data from a different measurement station, was compiled from the Swedish Meteorological and Hydrological Institute (SMHI). The topography data of the area was provided by SWECO in the form of a Digital Elevation Model (DEM). This DEM was used within QGIS to extract the shape of FLS.

To collect more data for the model, a total of five field expeditions were conducted at the site. The first one, a reconnaissance, took place on the 15th of November 2019. The middle three of the expeditions concerned the installation and monitoring of water level loggers in the lagoon. The data obtained was used for the calibration and validation of the model. The final expedition, which took place on the 10th of December 2019, measured the bathymetry of large parts of the lagoon.

IPH-ECO was chosen as the software used to model water exchange in the FLS. Several modifications to the source code were done to adapt the software for the conditions found in the lagoon. These conditions pertained mostly the transient wet and dry processes found in the lagoon. As IPH-ECO is written in Fortran, the use of Microsoft Visual Studio was vital to access, edit and compile the source code. The use of other complimentary software was also vital during the entire process of creating and calibrating the model. These complimentary software included VisIt, Notepad++, SQL Database Studio and HOBOware PRO.

After calibrating and validating the model, simulations could be run. The results from various simulations was used to gain a deeper understanding of the water exchange processes found in the lagoon. The simulations covered a period of two months. QGIS and MATLAB scripts were used to process the results.

2 Coastal Lagoons and Related Processes

This chapter provides information about lagoons, water exchange, sea level variations and sediment transport, among other, with the purpose of providing the reader with the necessary knowledge to understand the theoretical basics of this thesis.

2.1 Coastal Lagoons

Coastal lagoons occur in the transitional zone between sea and land, constituting water bodies that are connected to the sea by one or several channels known as inlets, see Figure 1. Lagoons are shallow water bodies with depths seldom exceeding a few metres, though this can vary depending on the sea level.

Figure 1: Example picture of a lagoon. The picture depicts the Ölüdeniz lagoon in Turkey (Maxar Technologies, 2020).

Around 13% of coastal areas worldwide consists of coastal lagoons and most of them were formed during the Holocene as a result of sea level rise and generation of coastal barriers by marine processes. In terms of geological timescales, lagoons have a short life span and can rapidly vanish due to sediment infilling (Kjerfve, 1994).

The ecosystems of lagoons are often unique and functions as a habitat for many animal species. Should the water quality in the lagoon not be sufficient, then a significant impact on the aquatic life and the ecosystem could be expected (Kjerfve, 1994).

According to Kjerfve (1994), lagoons can be classified into three different categories depending on their connection to the ocean. The three different categories are choked, restricted and leaky lagoons. These categories are illustrated in Figure 2.

Choked Lagoons are lagoons with only one inlet, with a cross sectional area significantly smaller than the area of the lagoon. The narrow inlet works as a filter, reducing the tidal

amplitude and water level fluctuations within the lagoon (Kjerfve, 1994). Thus, the tidal prism in a choked lagoon is smaller in comparison to restricted or leaky lagoons. The tidal prism or tidal volume is defined as the mass of water exchanged between the sea and lagoon during one tidal cycle, and is roughly calculated as the surface area of the lagoon multiplied by the tidal range:

$$\Delta V = A_{lagoon} \cdot (h_{flood} - h_{ebb}) \tag{1}$$

where V is the water volume of the lagoon, A_{lagoon} is the area of the lagoon, h_{flood} is water level during flood tide and h_{ebb} is the water level during ebb tide.

Restricted Lagoons are defined as large water bodies connected to the ocean by two or more inlets. Consequently, the flushing times are shorter in comparison with choked lagoons due to well-defined tidal circulation and influence from winds. The definition of flushing time is discussed in chapter 2.3.2.

Leaky Lagoons are water bodies with many connected inlets, providing adequate water exchange with the ocean. Tidal currents are strong enough to counteract both the littoral drift and wave actions. Both of these phenomena tend to close the inlets (Kjerfve, 1994). The effects of littoral drift and wave actions are explained in chapter 2.5.

Figure 2: Drawings illustrating the different classification of lagoons (Kjerve, 1994)

2.2 Water Balance

Understanding the net water balance of a lagoon is important in order to analyse the lagoon processes and characteristics. The net water balance can be defined as a mass conservation equation which describes the different fluxes. The equation is given by Miller et al. (1990) as:

$$\frac{dV}{dt} = P - E + D + G + A \tag{2}$$

where V is the volume of the lagoon, $\frac{dV}{dt}$ describes the change in storage over time, P is the rate of precipitation, E is the rate of evaporation, D is the freshwater discharge, G is the groundwater seepage and A is the advective gain or loss of water through a transverse cross-section.

2.3 Water Exchange

The water exchange in a lagoon can be defined as the amount of water flowing into the lagoon and the amount of water flowing out over a fixed period of time. The water exchange depends on several factors such as wind, tides, waves, evaporation, and river flows. Additionally, geometrical properties such as the shape and size of the lagoon, inlet dimensions and bathymetry contribute significantly to the water exchange (Miller et al., 1990).

In a lagoon, water exchange can be evaluated in different manners and timescales. Terms like residence time, renewal time and flushing time are often taken into consideration when discussing the water exchange between a lagoon and the sea. In this thesis, emphasis is put on flushing time and residence time. These two concepts are explained in chapters 2.3.2 and 2.3.3.

2.3.1 Lagoon Circulation and Mixing

As stated by Miller et al. (1990), lagoon mixing depends on various factors such as wind speed, tidal variations and mixing due to gravitational forces caused by temperature and salinity differences. The wind effect can cause wave action in the lagoon which subsequently leads to vertical mixing. Since lagoons are often shallow, this vertical mixing can extend to the bottom, resulting in vertical homogeneity. Vertical stratification due to differences in salinity and temperature, with denser water sinking to the bottom, might evolve during low river inflow (Kjerfve and Magill, 1989). In shallow lagoons, horizontal stratification is more common. This has an impact on the circulation inside the lagoon. As shown in Figure 3, wind mixing occurs when surface water is pushed downwind, forcing it to circulate along the bottom as it hits the edge of the lagoon.

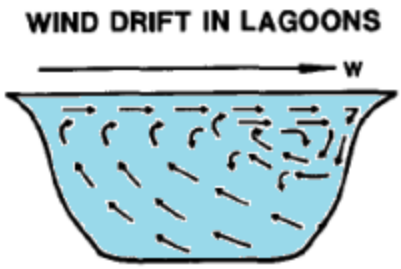

Figure 3: Principal sketch of wind forced mixing (Kjerfve and Magill, 1989).

Wind effects on a lagoon can be divided into local effects, which includes wind-driven currents, short period waves, setups along with setdowns, and far-field wind effects such as oscillations in sea level. Far-field wind effects results in slow variations of the lagoons water level and during infilling low-lying parts around the lagoon can become inundated (Kjerfve and Magill, 1989).

2.3.2 Flushing Time

Estimating the time scales of water exchange in a lagoon can be performed by analysing the flushing time. According to de Brito Jr. et al. (2017), flushing time is used to evaluate the water exchange and water renewal of the entire water domain without addressing the importance of underlying physical processes. The flushing time can simply be defined as:

$$T_f = \frac{V}{Q} \tag{3}$$

Where T_f is the flushing time, V is the volume of the water domain and Q the volumetric flow rate through the system.

However, the water in a domain is regarded to never be completely renewed. Thus, in this report, the flushing time is defined as the average time of which a water parcel spends in the system. According to de Brito Jr. et al. (2017), the domain of water can be compared as a continuously stirred tank reactor (CSTR). The concentration decay in a CSTR is defined as:

$$C(t) = C_0 e^{\frac{-t}{T_f}} \tag{4}$$

Where $C(t)$ is the concentration at a certain time and C_0 is the initial concentration. To use the simplification of conceptualizing the water domain as a CSTR, some assumptions must be clarified:

1. A known load of tracers must be dropped into the water domain producing a homogeneous concentration C_0 when t=0.

2. This must be spread out over the whole region of water through immediate and thorough mixing.

3. There may not be variations in volume or flow in the water domain.

4. Ultimately, no further load of tracers should be dropped after the initial introduction of tracers.

A so-called e-folding flushing time as mentioned by de Brito Jr. et al. (2017), can be calculated. This is defined as the time for the average tracer concentration to decrease to e^{-1}= 37%, hence the name. A Lagrangian particle tracking, LPT, is used and the particles are assumed to have the same density as the fluid, i.e neutral buoyancy.

2.3.3 Residence Time

The concept of residence time is used to estimate the time it takes for a Lagrangian water parcel on a specific location to leave a water body for the first time (Delhez et al., 2014). The boundary by which the parcel is considered to be out can be decided for the specific situation and is usually set near a hypothetical discharge location. The residence time can be analysed for both re-entrant water parcels and non re-entrant water parcels. A re-entrant water parcel is defined as a water parcel that leaves and then re-enters the water body. The water parcels provide an opportunity to evaluate the influence of the inlet on the residence time and conduct a water exchange assessment. According to Rynne et al. (2016), the birth time for a water particle is defined as the time when it enters the water domain and the age is defined as time spent inside the system as shown in Figure 4. Age can also be used as a measure to assess the renewal of water. At every specific time, every individual water particle has a specific age. To physically track the movement by using tracers in the field is thus merely an approximation of the residence time. Evaluation of residence time can be performed by utilizing a calibrated hydrodynamic model of the water domain, with the possibility to use higher quantities of artificial tracers in the simulation. Residence time is a useful tool of measurement in situations such as the restoration of water domains where the quality of water is insufficient (Delhez et al., 2014).

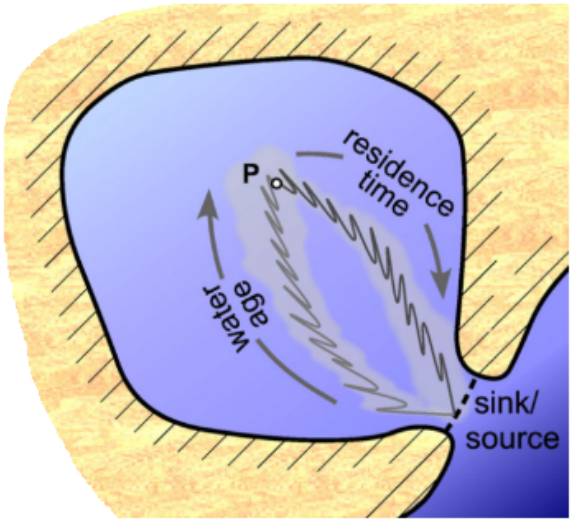

Figure 4: A principal sketch illuminating the concept of residence time and water age. Residence time is the time it takes for a water parcel to leave the water domain. Water age is the duration by which the water parcel has been in the domain (Viero and Defina, 2016).

2.4 Sea Level Variations

Local sea level variations are driven by tidal and non-tidal forces. Tidal forces comprise the gravitational pull that both the sun and the moon have on the Earth's water surface. Depending on the location of them both, spring or neap tides can occur. Non-tidal forces refers to the coastal winds, air pressure, periodic oscillations, Coriolis force and frictional forces that raise or lower the local sea water levels (Miller et al., 1990).

The oscillating tidal force usually have a 12 or 24 hour time scale, e.g. high and low tide is reached, sometimes several times, within that interval. A semi-diurnal tidal cycle (12 hours) is prevalent along the North Atlantic coast. Meteorological phenomenon such as coastal winds have a more extensive timescale. This timescale could be upwards of a week.

2.5 Littoral Sediment Transport

Littoral sediment transport is a natural coastal phenomena occurring due to processes near the littoral zone such as waves, wind, currents and tides. The sediment transport can be divided into two groups; longshore sediment transport and onshore-offshore sediment transport (US Army Corps of Engineers, 1984).

Onshore and offshore sediment transport has a direction perpendicular to the coastline and occurs when waves transport sediment grains on the bottom as they traverse shallow water. This kind of sediment transport exhibits a significant seasonal variation and the beach width is increased during the summer and eroded during winter (Hanson and Larson, 1993).

The longshore sediment transport is typically caused by offshore waves generated by wind. When these waves strike the coastline at an oblique angle, longshore currents are formed. Stirred up sediment, generated by the breaking waves, is transported along the coastline by these currents. This could have a considerable impact on long-term changes of the coastline (US Army Corps of Engineers, 1984). The extent of suspended material depends on the

breaking type of the wave. Plunging waves has a greater ability to stir up sediment than other types of waves. The direction and velocity of longshore currents as seen in Figure 5, are determined by the wave breaker height and the incoming wave crest angle. The height and angle assumes different values depending on the time and the seasons of the year. This also results in the shoreline adopting different shapes over time. The angle between the coastline and wave crest is the factor which has the greatest impact on the longshore current velocity (US Army Corps of Engineers, 1984).

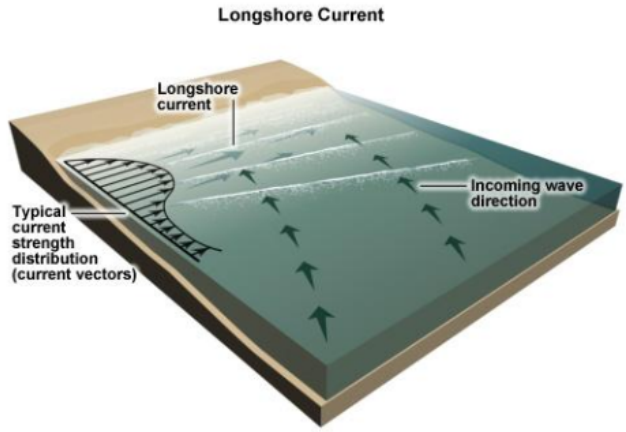

Figure 5: Location of longshore currents and how they are created by incoming waves striking the beach at an oblique angle (U.S. Geological Survey, 2012).

When looking at a section of the coastline, there will be transport of sediments to the left (Q_L) or to the right (Q_R) of this section. As described by Davidson-Arnott (2010), the net longshore transport, Q_{net}, is equal to the difference between the transport of sediments to the right and to the left according to:

$$Q_{net} = Q_R - Q_L \tag{5}$$

Gross sediment transport is the sum of the transport from the left and the right, and is defined as the total sediment transport regardless of direction as:

$$Q_{gross} = Q_R + Q_L \tag{6}$$

The net longshore transport rate defines the sediment transport in a predefined direction, and can be used to predict the coastal evolution on open coastlines and to facilitate the work when designing protected inlets (Davidson-Arnott, 2010). Awareness of sediment transport directions can be crucial to avoid unwanted accretion on the updrift side or erosion on the downdrift side adjacent of an artificial structure. However, measurement of longshore transport rate and direction is expensive and challenging. The gross sediment transport could for example be evaluated to find out how often a lagoon inlet has to be dredged (Hanson and Larson, 1993).

2.6 Inlet Dynamics

Tidal lagoon inlets are exposed to shifting tidal currents depending on the hour of the day. These currents are generated by the tide when the water level at one side of the inlet is higher

than the other side. Consequently, water flows from the higher elevation to the lower. The tidal sea level variations has a timescale of 12 to 24 hours. The force of the water flow through a lagoon inlet is not merely based on the tide. Water level differences between the sea and lagoon due to meteorologic weather phenomenons and sea level oscillations also occurs with a timescale of several days (Danish Hydrological Institute, 2018). During ebb tide the tidal current is directed from the lagoon towards sea, and during flood tide the tidal current is directed the opposite way (Danish Hydrological Institute, 2018).

The tidal current is accountable for the transport and exchange of sand between the littoral zone and the lagoon, creating formations of offshore shoals and lagoon shoals, also known as ebb shoals and flood shoals. During ebb shoals, sand is carried through the inlet and accumulated on the ocean side of the inlet. The flood shoal is affected by the flood currents. Sand is carried and accumulated on the side of the inlet facing inland instead (US Army Corps of Engineers, 1984). An example of a lagoon inlet can be seen in Figure 6.

Figure 6: Picture of the inlet at the Esquimalt lagoon in Canada. Note the accumulation of sediment (TerraMetrics, 2020).

Furthermore, the longshore transport of sediment due to the longshore current has an impact on accumulation of sand around the inlet. Wave generated currents continuously push sand into the inlet area, while the inlet flow generated by tide and wind carries the sediment seaward or into the lagoon. The stability of the inlet depends on the relationship between these opposing forces (US Army Corps of Engineers, 1984). An inlet could possibly close during storms due to significant sediment transport. Should the sediment transport block the inlet and disrupt the water exchange in the lagoon, then it is possible to alleviate this by dredging the inlet.

As Figure 15 shows, sand transport typically leads to shifting locations and varying depths of the inlet across a period of time. Migration of the inlet depends on different factors such

as sediment supply, tidal prism and wave energy (US Army Corps of Engineers, 1984). The cross section of an inlet varies, with usually the highest water velocities being reached around the throat of the inlet where the cross section is the smallest.

3 Flommen Lagoon System

This chapter presents information about the study area of the FLS, located on the west coast of the Falsterbo Peninsula. A general overview of the area, along with its climatology, geology and coastal processes is provided below.

3.1 Overview

The Flommen Lagoon system is located on the western edge of the Falsterbo Peninsula between the latitudes 55°23'12"N and 55°24'56"N and longitudes 12°49'09"E and 12°50'22"E. The Falsterbo Peninsula is in turn located in the southwestern part of the Swedish province of Scania and is known for its unique nature, dazzling beaches and substantial value of historic picturesque buildings. See Figure 7 for a region-wide map of Scania.

Figure 7: Map showing the location of the Falsterbo Peninsula in the province of Scania (Google, 2019).

The FLS is the only lagoon system in Sweden. Its ecosystem hosts migrating birds and one of the largest population of European green toads, natter jack toads and sand lizards in Sweden (Länsstyrelsen, 2019). The entire lagoon system is classified as a nature preserve by European and Swedish authorities. Hence, the water quality in the lagoon system is of great importance and has become a matter of concern. Figure 8 offers a ground-view of the lagoon system.

Figure 8: Picture of the Flommen Lagoon system. View of a channel pointing towards the south. Photo by: Kristian Ångbäck

Likewise, flooding problems in the adjacent area of the Flommen Lagoon system, including the local golf course, has troubled the area. To prevent flooding, sluice gates at the inlet Slusan were constructed in 2016. These gates are manually closed when the local sea level reaches 0.5 m and above. See Figure 9 for a view of the gates. Furthermore, the construction of the gates provide a threshold of -0.35 m for the minimum water level. Thus, should the sea water level decrease to less than -0.35 m, then the flow between the sea and the lagoon will cease. These water levels are expressed using the height reference system RH2000.

Figure 9: Sluice gates at Slusan. Photo by: Kristian Ångbäck

As noted by Davidsson (1963), the Falsterbo Peninsula is an example of a distinct coastal formation named "complex tombolo". Essentially, a complex tombolo consists of several island kernels joined together with the coastline. This can be seen in Figure 10.

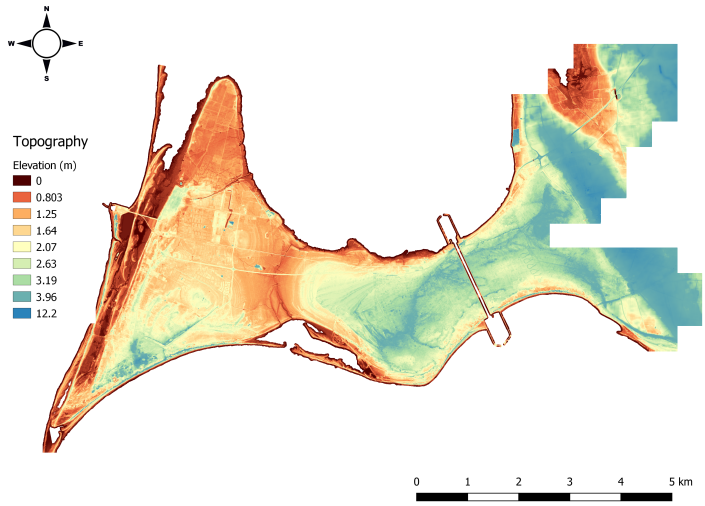

Figure 10: Digital Elevation Model (DEM) of the Falsterbo Peninsula provided by SWECO (2019). Post-processing conducted in QGIS to make different elevations more visually distinct. Heights are expressed in RH2000.

Figure 11: Satellite imagery showing the Flommen Lagoon system and neighbouring town of Skanör-Falsterbo (TerraMetrics, 2019)

As seen in Figure 11, Flommen Lagoon has an elongated shape that stretches for approximately 3.3 km, and covers an area of roughly 2.6 km^2. Flommen Lagoon only has one inlet, Slusan. Slusan acts both as an inlet and an outlet depending on the meteorological and tidal forces at play. This inlet can be seen in detail in Figure 12. The lagoon is also characterised by narrow channels, with widths under 20 m. These channels tend to become even more

restricted as they extend further into the lagoon. At its most narrowest, the channels barely extend to a width of 5 m.

Figure 12: Composite satellite imagery of the Flommen Lagoon system and the Slusan inlet (TerraMetrics, 2019).

There is very limited river discharge into the lagoon system and the influence of drainage to the system is negligible. However, it has been noted in an internal report by SWECO (see Appendix 12.4) that the salinity and chloride concentration varies throughout the lagoon. Usually the water in the southern part of the lagoon has slightly lower salinity than the seawater entering through Slusan. This likely implies possible groundwater infiltration. But given the lack of data and research regarding this groundwater infiltration, it is not further elaborated upon in this thesis.

3.1.1 Climatology

Due to its location, at the most southern edge of the most southern province in Sweden, the lagoon system has a temperate oceanic climate (Kottek et al., 2006). This implies warm summers with daily mean temperatures not exceeding 19 °C and cool winters with mean temperatures not sinking below 1 °C (Swedish Meteorological and Hydrological Institute, 2019*b*). Its temperate oceanic climate also implies a relatively equal distribution of precipitation throughout the year. Monthly precipitation average around 42 mm (Swedish Meteorological and Hydrological Institute, 2019*a*). Local data on evaporation are unavailable, necessitating the use of regional data as a substitution. Thus, the evaporation rate is assumed to be 500 mm/year.

3.1.2 Geology

As described by Hanson and Larson (1993), the geological state of the Peninsula, including the FLS, is dominated by deposited sand sediments resting on a layer of moraine clay. This layer of moraine clay rests in turn on a bedrock of limestone. A drawing of this can be seen in Figure 13. The Falsterbo Peninsula is a relatively young geographical formation. A post-glacial formation, its foundation emerged not more than 6000-7000 years ago (Blomgren, 1999).

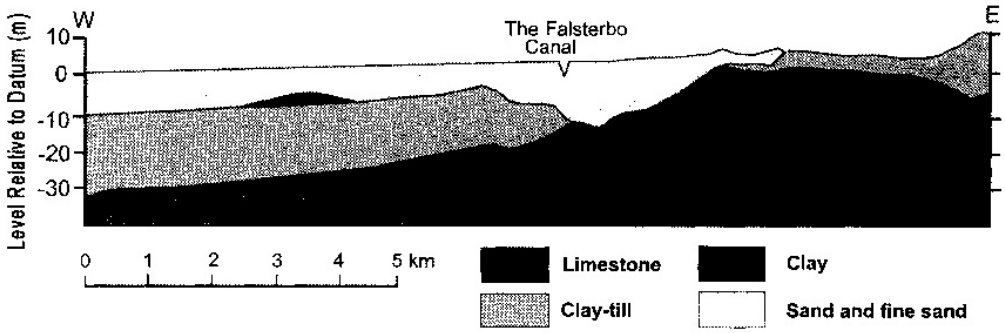

Figure 13: Schematic cross section of geology at Falsterbo Peninsula in the east to west direction (Blomgren and Hanson, 2000).

3.2 Local Water Exchanges and Coastal Sedimentation

The water system in Flommen relies on water exchange from Öresund. At the present, this water exchange is solely enabled by the narrow tidal inlet Slusan. This makes the Flommen Lagoon a choked lagoon. The inlet is located on the part of the coastline that is gradually moving seaward (Blomgren, 1999). This coastline movement is due to longshore sediment transport being blocked by the protruding Skanör Harbour on the northern side of the lagoon. As described in chapter 2.5, this type of increasing beach width in front of a structure indicates a high net sediment transport, Q_N, in the northern direction.

Apart from brief mentions from Blomgren (1999) and a study on inlet sedimentation from Danish Hydrological Institute (2018), further data on water exchange inside the FLS are non-existent.

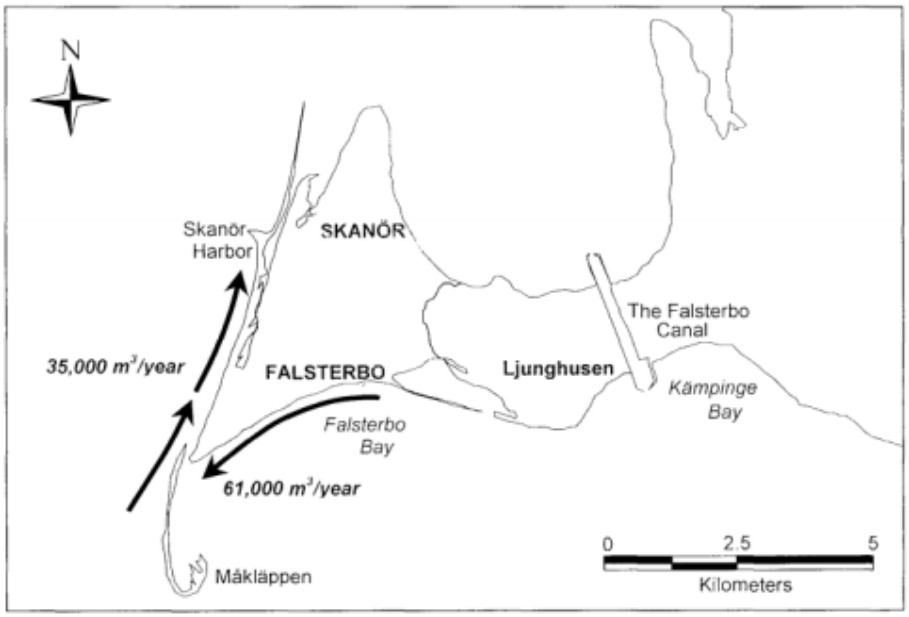

Figure 14: Map by Hanson and Larson (1993) of the Falsterbo Peninsula, displaying the estimated net sediment transport.

As seen in Figure 14, Hanson and Larson (1993) estimated the net sediment transport along the west coast to be around 35.000 m^3/year in the northbound direction. It is highly likely that the inlet is blocked when the sand transport is high, for example during storm events. The limited tidal flow and wind-induced flow at the FLS is not adequate to keep Slusan open (Danish Hydrological Institute, 2018). See Figure 15 for examples of the sedimentation near Slusan. For a ground view of Slusan, examine Figure 16.

Figure 15: Picture of the inlet Slusan in Flommen Lagoon showing the varying geometry and location of the inlet (Maxar Technologies, 2019).

Figure 16: Picture of the inlet Slusan, view towards the sea. Note the accumulation of sediment at the entrance. Photo by: Kristian Ångbäck

Coastal sedimentation threatens to block Slusan. This would disrupt the water exchange in the FLS and the ecosystem residing inside it. Thus, dredging of the inlet is reguarly carried out to prevent blockage (Danish Hydrological Institute, 2018). Sedimentation at Slusan is caused by a sandy barrier that is formed by the northbound littoral drift and accretion south of Skanör Harbour. As mentioned by Hanson and Blomgren (2000), the construction of Skanör Harbour has caused considerable changes in the sediment transport patterns, also affecting the neighboring shoreline north of the harbour with noticeable coastline erosion. Figures 17 and 18 showcases the erosion around the Skanör Harbour.

Figure 17: Map from 2007 showing Slusan and the neighbouring coastline around the Skanör Harbour (Maxar Technologies, Lantmäteriet/Metria and NASA, 2019). The red line highlights the 2007 coastline.

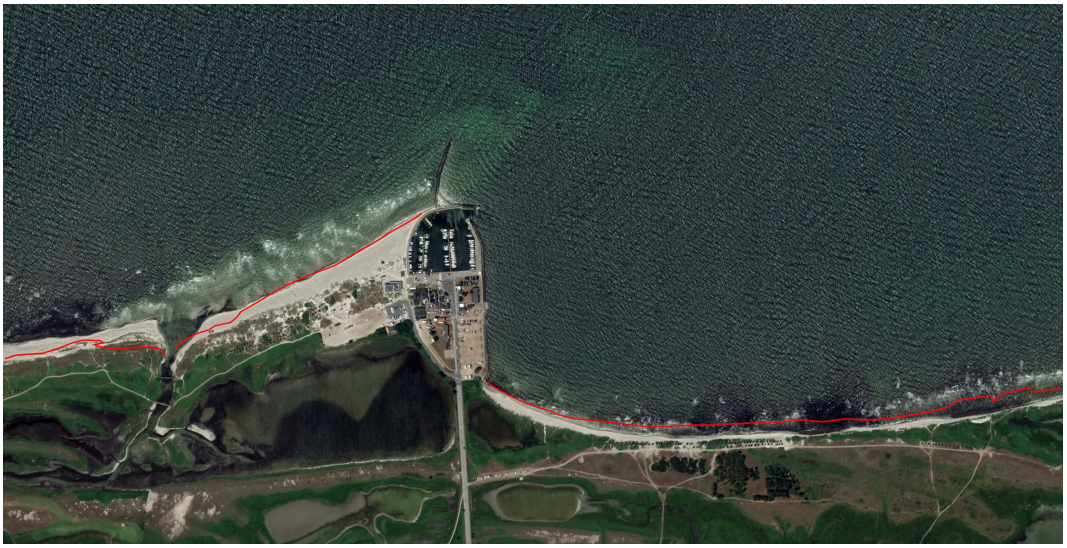

Figure 18: Map from 2019 showing Slusan and the neighbouring coastline around the Skanör Harbour (Maxar Technologies, 2019). The red line denotes the 2007 coastline. Note the sedimentation south of the harbour, and the general coastline erosion north of it. A part of the northern coastline, directly adjacent to the harbour, remains unaffected.

By comparing aerial images from 2007 and 2019, the Danish Hydrological Institute (2018) drew the conclusion that the area south of the Marina saw a general shoreline advance of 1 - 2.5 m a year. It should be noted that the area around Slusan sees an exceptionally high rate of deposition, at around 4 m a year. The area north of the harbour instead sees an shoreline erosion of roughly 1 m a year. However, a part of the shoreline in the direct

northern vicinity of the harbour, is relatively unaffected by the erosion. These findings are further corroborated by Hanson and Larson (1993).

3.3 Wind Climate

Figure 19: Location of the wind gauge south of the FLS (Swedish Meteorological and Hydrological Institute, 2020*a*).

Based on data from a SMHI weather station located south of the FLS (see Figure 19), at the latitude 55°23'0.96"N and longitude 12°49'13.08"E, a wind rose illustrating the prevailing wind direction and intensity at the FLS was generated (see Figure 20). It shows that the dominating wind direction is between the northwest and the southwest with an average wind speed of around 6 m/s, as seen in Figure 21. The wind data is based on 30 years of observations between 1988 and 2018. Measurements consisted of the average wind speed covering 10 minutes every third hour.

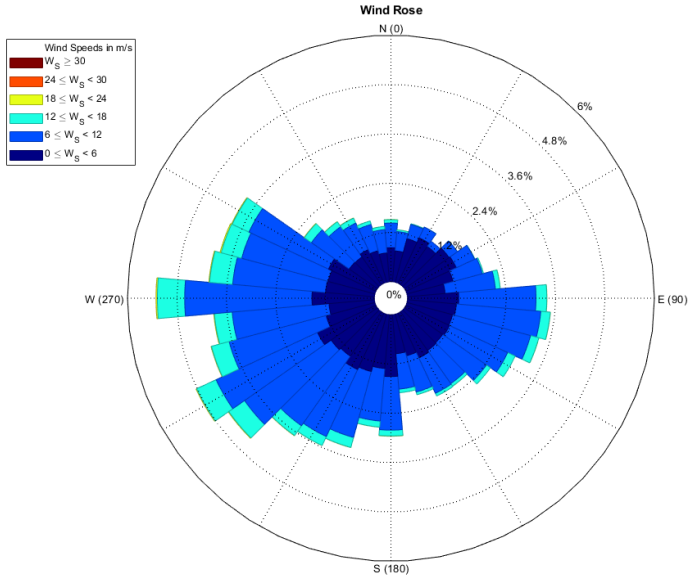

Figure 20: Wind rose illustrating wind direction and intensity, based on measurements from SMHI between 1988-2018.

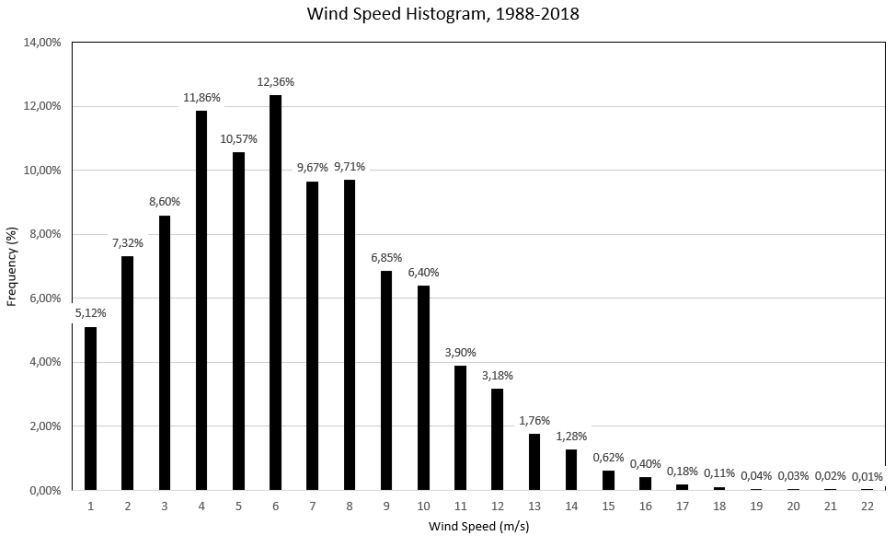

Figure 21: Wind histogram for the period 1988-2018. Note that wind speeds above 15 m/s are exceedingly rare. Only once during the 30-year wind measurement period did the wind speed reach storm wind speeds i.e. 25 m/s (Swedish Meteorological and Hydrological Institute, 2020*a*).

3.4 Wave Climate

The seaward movement of the shoreline south of the harbour along with the erosion of the coastline north of it, can be explained by the dominant direction of the wave climate (Hanson and Larson, 1993). Most of the waves reaching the western end of the Falsterbo Peninsula originate from the west or the southwest. The wave climate has the biggest influence on the sediment transport.

3.5 Water Balance in Flommen

Flommen has negligible fresh water discharge, as its sole outlet is the saltwater outlet Slusan. Neither are there any significant freshwater inlets leading into the lagoon system. As for the groundwater infiltration, it is disregarded partly to simplify the model calculations, and partly because there is no available data. Groundwater infiltration is assumed to play a relatively minor role in the water balance in comparison with advective gain and loss.

Thus, the water balance in Flommen Lagoon is defined as:

$$\frac{dV}{dt} = P - E + A \tag{7}$$

where $\frac{dV}{dt}$ describes the change in storage over time, P is the rate of precipitation, E is the rate of evaporation and A is the advective gain or loss of water through a transverse cross-section.

3.6 Water Levels

All the water level measurements in this thesis are based on the height reference system RH2000. Data from Swedish Meteorological and Hydrological Institute (2020*b*) on water levels between 2009-2019 in Skanör-Falsterbo reveals a water level fluctuation of $\pm$ 0.5 m in the harbour and a mean annual water level of 0.173 m. The sea level measurement station run by SMHI is located in the Skanör Harbour, 55°25'0.12"N and 12°49'45.84"E, as shown in Figure 22. The water level fluctuation near Slusan is assumed to be the same due to its proximity to the marina.

The most distinguished fluctuation in water level has a time scale of several days. This implies that most of the fluctuation is caused by meteorological forces. Strong winds in the coastward direction can cause set-ups which generates an increased water level near the coast (Swedish Meteorological and Hydrological Institute, 2014). This creates a slope in sea level from one side of the sea to the other. When the wind direction changes, the sea level reverts to its regular flat shape, causing a sea level oscillation. The time between the two peaks of the oscillation varies and is governed by the water depth as well as the expanse of the sea. According to Swedish Meteorological and Hydrological Institute (2014), oscillations between the Gulf of Finland and the southwestern Baltic has a period of 27 hours and oscillations between the north and south of the Baltic Sea has a period of 4 days.

If the fluctuation was mainly caused by tidal forces, then it would have a time scale of 12 or 24 hours instead. This is further corroborated by Hanson (2007), which states that the tidal range in the adjacent Baltic Sea is less than 0.25 m. Thus, tidal fluctuation is practically non-existent near Falsterbo Peninsula and Flommen Lagoon.

Due to water level differences between Kattegatt and the south of Baltic Sea, large currents are created, which has a small affect on the transport of sediment (Hanson and Larson, 1993).

According to Hellström (1941), sea level variations in the Baltic is caused by several factors. These include tidal forces, river discharge, precipitation and water exchange between Kattegatt and the Baltic Sea.

Water level fluctuations in the lagoon basin are currently unknown and are investigated in this thesis.

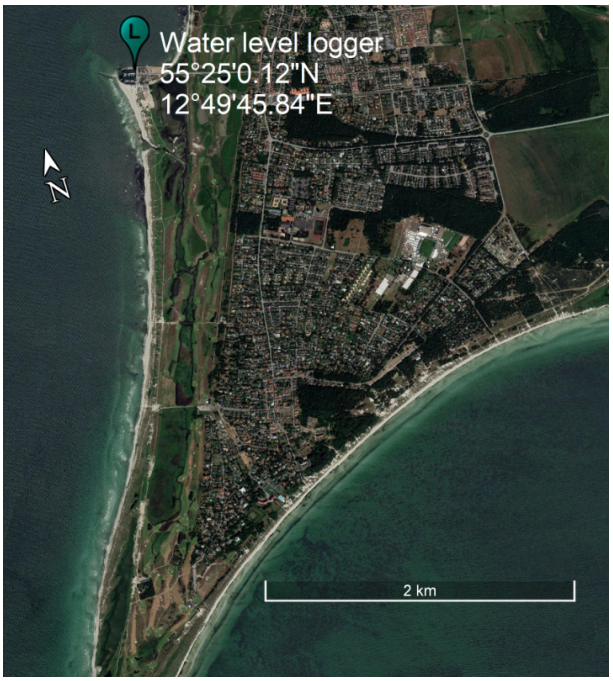

Figure 22: Location of the sea level measurement station north of the FLS (Swedish Meteorological and Hydrological Institute, 2020*b*).

4 Field Measurements

In this chapter, the measurements collected to create a calibrated and validated model of the lagoon are presented. Previous studies, measurement procedure and collected field data are also discussed.

4.1 Previous Studies

Studies on the bathymetry and water exchange of Flommen Lagoon remain scarce. The only past study conducted on Flommen Lagoon within those fields is that of Wang (2019). In the cited paper, measurements on bathymetry were mostly carried out in the northwestern part of the lagoon and Slusan. Some measurements were conducted in the central parts of Flommen, but these measurements were too scarce to be reliable enough for use in this thesis.

4.2 Equipment

Essential to calibration and validation of the model was data collection of varying water levels and bathymetry of the lagoon. To accomplish this task, the main equipment used were two HOBO U20L Water Level Loggers and one SPS985 GNSS Smart Antenna. The processing of logger data was done on a computer using the HOBOware PRO software. For additional information on the equipment, please refer to Appendix 12.1, 12.2 and 12.3.

4.3 Measurement Procedure

Two HOBO U20L were installed in Flommen Lagoon. As seen in Figure 23 they were attached to bridge piers. One water logger was embedded in the northern part of the lagoon, and the other one in the southern part. The associated coordinates were 55°24'22.26"N , 55°49'50.32"E and 12°23'55.82"N, 12°49'40.25"E respectively. A map with the locations of the loggers can be seen in Figure 24.

The loggers collected data from the 20th of November 2019 to the 5th of December 2019. The northern logger spent one week recording data. It was then detached and its database uploaded. It was then reattached to the bridge pier. Hence, there is an one hour gap in the data recording stored in northern logger. The southern logger spent two weeks recording uninterrupted. The loggers operated with a 15 minute data sampling frequency.

The distance between the water surface and the top of the bridge was measured at the start of each deployment. This distance was vital for the calculation of the starting water level, measured in RH2000, at the start of both deployments. The height of the bridge was also measured after the loggers had been detached by using the GNSS receiver. Thereafter, the recorded data found in the loggers could be fixed to the correct reference level.

The water loggers do not actually measure water levels, but instead changes in absolute pressure. In conjunction with air pressure data supplied from a nearby SMHI weather station and an reference height, data containing fluctuations of absolute pressure from the loggers can be converted to data containing fluctuations on water levels.

Figure 23: A picture showing the deployment of a water logger. The water logger is deployed by attaching it to a bridge pier. Photo by: Kenny Lay

Figure 24: Position of water loggers in the FLS.

To collect data on the field bathymetry, a field expedition was conducted on the 10th of December 2019 using the SPS985 GNSS Smart Antenna. Previous measurements of the bathymetry focusing on the northwestern part of the lagoon had been collected by Wang (2019), but these measurements do not extend into the narrow channels that run in the southern direction from Slusan. During the field expedition, measurements were conducted by walking and wading through the lagoon system, measuring the bathymetry with an approximate sampling distance of around 10 meters. Cross section measurements were performed regularly. The location of these measurements, together with those of Wang (2019) can be seen in Figure 27. The field expedition was unable to collect data on the northeastern part of the lagoon due to the prevalence of what seemed to be nesting birds in that area. Due to the disturbance on the nesting grounds the expedition would have, the decision was made to not proceed. Figure 25 shows the field expedition conducting measurements in the FLS.

Figure 25: Bathymetry measurements carried out in Flommen by using a SPS985 GNSS Smart Antenna. Photo by: Clemens Klante

4.4 Collected Data

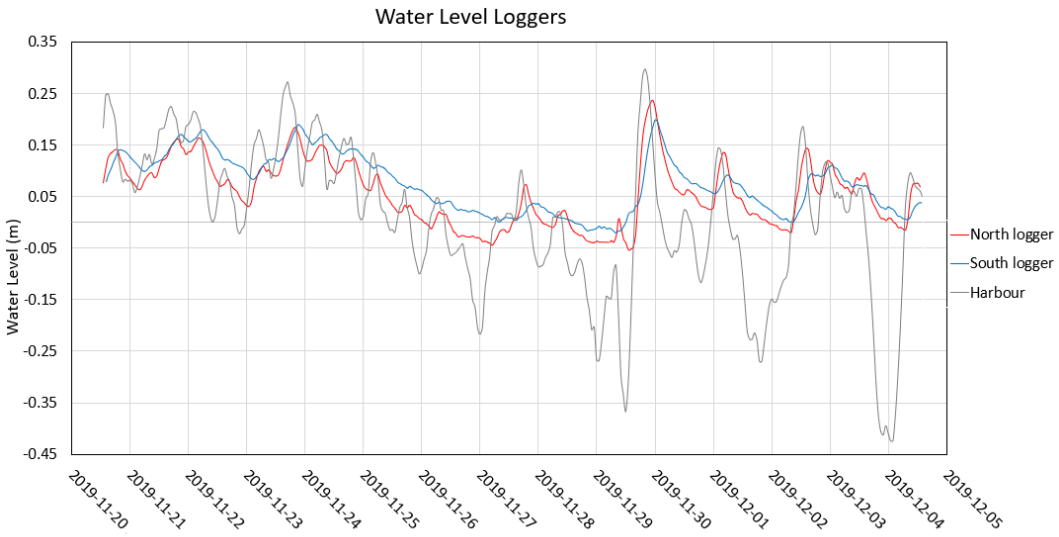

Figure 26: A graph of the water level between the 20th of November 2019 and the 5th of December 2019, measured by the north and south logger. Harbour water level is also visible for comparison.

Figure 26 displays how the water levels varies in the northern and southern parts of FLS in regards to the sea water level. It is possible to infer that there is a clear time lag between the water level in the lagoon and the sea. The delay between water level peaks for the north logger and the sea water level is around 2 hours, and approximately 4 hours for the south logger. Consequently, a dampening effect can be observed between the sea water level and the lagoon, as the peaks recorded by both the north and south logger are reduced.

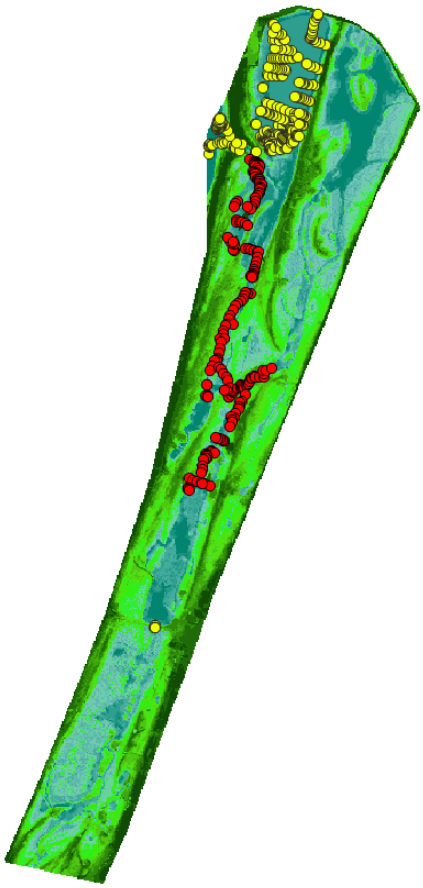

Figure 27: Stylised map of the FLS. The red dots are bathymetry measurements collected during the field expedition. The yellow dots are bathymetry measurements collected in a previous study by Wang (2019).

4.5 Sources of Errors

The data output from the water loggers could contain several sources of errors. One possible source can be found in the water loggers themselves. According to the HOBO U20L datasheet, the typical error when measuring water levels is $\pm$ 0.3 cm. Another potential source of error could be the measurements conducted in order to establish the water reference level. These were done by hand with a simple meterstick. There exists a few abnormalities in the logger data shown in Figure 26. There are brief instances of measurements that suggests the water level in southern part of the lagoon is rising, while the water level in the northern part is sinking. This is peculiar since the outlet is in the northern part of the lagoon. These strange

readings might have occurred due to measurements errors from the loggers.

In regards to the bathymetry measurements, the most likely source of error is the handling of the measurement equipment. Unless used with absolute mathematical precision, e.g. the measurement stick is held completely straight, then a measurement error, however insignificant, can be expected. The proper positioning of the stick in the vertical direction was somewhat problematic, since parts of the lagoon had layers of soft sediment. This would often cause the stick to sink down. Another source of error is the precision margin of the SPS985. Every measurement has a horisontal and vertical precision of roughly $\pm$ 0.05 cm respectively. This seems negligible in comparison with the other source of error just mentioned.

The short water level measurement data set is also a possible source of error. A longer measurement period would maybe have resulted in more reliable results.

5 The IPH-ECO Model

This chapter provides information about the software IPH-ECO used in this thesis. Furthermore, the governing model equations are also explained. In this thesis, IPH-ECO was used as a 2D vertically integrated software capable of modelling water exchange. It is also capable of modelling, if desired, salinity concentrations and nutrient transports in a lagoon.

5.1 IPH-ECO Model Description

There are other modelling software available, such as Delft and Telemac that are also capable of simulating water exchange to a similar extent as IPH-ECO. Another way to model water exchange is to use box models. One example of this can be found in a work by Wang (2019) that also dealt with the FLS.

IPH-ECO is a software based on a finite element procedure which can produce a three-dimensional complex dynamical model and is defined by the principle of conservation of mass and momentum. It can be adapted to also produce 0D, 1D and 2D models. The software is developed at the Instituto de Pesquisas Hidráulicas (IPH), in Porto Alegre, Brazil. It can be used to create complex models of reservoirs, rivers, lakes and lagoons. The model is composed of different cells created by a mesh generator, either with a unstructured or structured grid. A structured grid consists of equally sized quadratic cells whereas the unstructured grid is built up by triangular cells which can vary in size and can be more refined in areas of interest.

The program is divided into two modules that consists of various partial differential equations. Module one is a detailed hydrodynamic module, defining water levels and flows. Module two describes water quality and transport of nutrients such as phosphorus, nitrogen and biological material, which can be used to enhance understanding of the behavior of different ecosystems. If desired, these two modules can be run together.

IPH-ECO possesses a GUI, which lets the user dictate the complexity of the model and facilitate the modifications of different parameters. The source code of IPH-ECO is written in Fortran. As seen in Figure 28, IPH can be described as different blocks. A user interface allows the entry of input data such as grid data, hydrodynamic data and meteorological data. Different parameter values and boundary conditions can be specified for different scenarios.

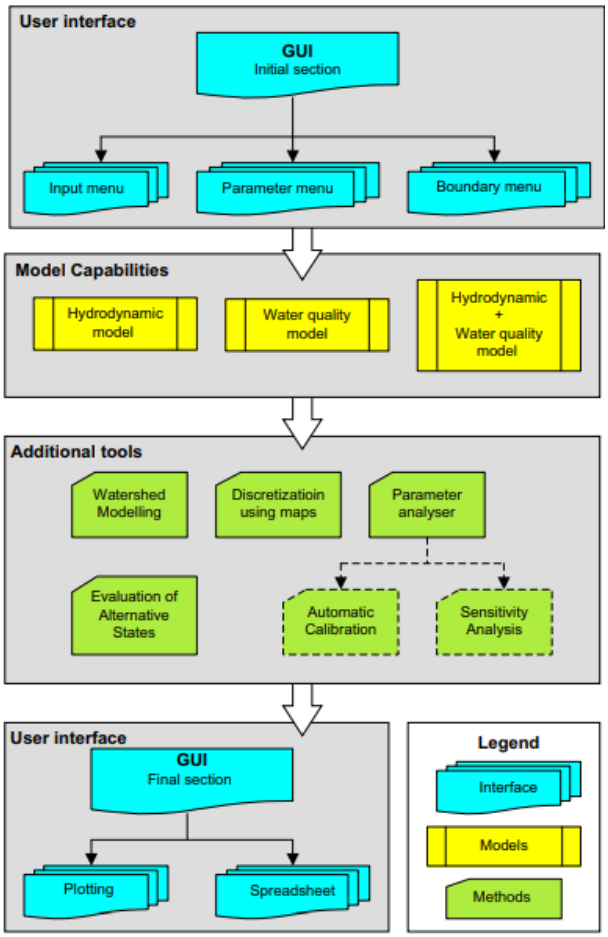

Figure 28: The 3 different blocks within IPH; User interface, model and additional tools (Fragoso et al., 2009).

5.2 Governing Model Equations

The composition of mathematical formulas within IPH-ECO is based on Navier-Stokes differential equations. These equations can be combined to form shallow water equations by assuming that horizontal flows are much greater than the vertical flows. To integrate the Navier-Stokes equations over a water column, IPH-ECO assumes two boundary conditions; wind stresses at the free surface and frictional forces at the bottom (Pereira et al., 2013). By using the momentum equations for an incompressible fluid with these boundary conditions, a term representing the divergence of stress along a water column can be produced as shown in equation 8 (Pereira et al., 2013):

$$A_v \frac{\partial u}{\partial z} = \tau_x - \gamma u \text{ and } A_v \frac{\partial v}{\partial z} = \tau_y - \gamma v \tag{8}$$

where A_v represents the vertical eddy viscosity, $\frac{\partial u}{\partial z}$ and $\frac{\partial v}{\partial z}$ are the horizontal velocity components along the water column, τ is the wind shear stress and γ is the friction on the bottom. The water velocity in the x- and y-direction are portrayed by u and v.

The momentum equations and continuity equation solved in IPH-ECO hydrodynamic module for a two dimensional situation according to Pereira et al. (2013) are:

$$\frac{\partial u}{\partial t} + u\frac{\partial u}{\partial x} + v\frac{\partial u}{\partial y} = -g\frac{\partial \eta}{\partial x} + A_h[\frac{\partial^2 u}{\partial x^2} + \frac{\partial^2 u}{\partial y^2}] + \tau_x - \gamma u + fu \tag{9}$$

$$\frac{\partial v}{\partial t} + u\frac{\partial v}{\partial x} + v\frac{\partial v}{\partial y} = -g\frac{\partial \eta}{\partial y} + A_h[\frac{\partial^2 v}{\partial x^2} + \frac{\partial^2 v}{\partial y^2}] + \tau_y - \gamma v + fv \tag{10}$$

$$\frac{\partial \eta}{\partial t} + \frac{\partial}{\partial x}\int_{-h}^{\eta} u\,dz + \frac{\partial}{\partial y}\int_{-h}^{\eta} v\,dz = 0 \tag{11}$$

where $v(x, y)$ and $u(x, y)$ are the velocity (m/s) in the horizontal x- and y-direction, t is the time in seconds, $h(x, y)$ is the water level relative to a chosen reference level in meter, η is the free surface level to an undisturbed reference level in meter. A_h is the horizontal eddy viscosity $(m^2 s^{-1})$ and f is the assumed constant Coriolis parameter (s^{-1}).

The horisontal eddy viscosity is calculated using a formula defined by Smagorinsky (1963):

$$A_h = \Delta x \Delta y \sqrt{\left(\frac{\delta u}{\delta x}\right)^2 + \left(\frac{\delta v}{\delta y}\right)^2 + \frac{1}{2}\left(\frac{\delta u}{\delta y} + \frac{\delta v}{\delta x}\right)^2} \tag{12}$$

The hydrodynamic module within IPH-ECO calculates the wind shear stresses (τ_x, τ_y) and bottom friction (γ), which are used as boundary conditions for the Navier-Stokes equations. Wind shear stress is proportional to the wind speed and is defined in equations 13 and 14:

$$\tau_x = C_D W_x \parallel W \parallel \tag{13}$$

$$\tau_y = C_D W_x \parallel W \parallel \tag{14}$$

where C_D is the wind stress coefficient, W_x and W_y the horizontal wind speed (m/s) and $\parallel W \parallel$ is the norm for the wind speed vector (m/s).

The bottom friction coefficient ,γ, within the module is defined as:

$$\gamma = \frac{g\sqrt{u^2 + v^2}}{C_v^2 H} \tag{15}$$

where H is the total water depth in meters as specified by $H = h + \eta$ and C_v is the Chèzy coefficient.

The Navier-Stokes differential equations previously discussed rely on Chèzy coefficients and not Manning coefficients. In an effort to be consistent throughout the modelling, the decision was made to apply Chèzy coefficients in place of Manning coefficients when calculating roughness. As soil roughness is usually expressed in Manning coefficients, an equation is needed for the conversion between each of the two. This equation is defined by Manning (1891) as:

$$C = \frac{1}{n} R^{\frac{1}{6}} \tag{16}$$

where C is the Chèzy coefficient, n is the Manning roughness coefficient, R is the hydraulic radius. In IPH-ECO, R is defined as the water depth. Do note that R has a low sensitivity due to the $\frac{1}{6}$ exponent attached to it.

A constant Chèzy coefficient is applied to the whole grid, despite the fact that the water depth is usually not fixed but in a state of constant state of flux. This is due to the limitations of the software which necessitates the input of a fixed Chèzy value to each individual cell.

6 Modelling Water Exchange

This chapter presents information about the setup and the application of the modelling software IPH-ECO needed to obtain a working hydrodynamic model of the FLS. The setup of the model, various input data and modifications of the model is discussed.

6.1 Model Setup

6.1.1 Reference System

A Cartesian coordinate system, with longitude (X-coordinates) and latitude (Y-coordinates), was used to define the area evaluated in the model. The reference system used in the model is SWEREF 99 TM (SWEdish REference Frame 1999, Transverse Mercator). The reference system was important to define in the initial phase of the thesis. The DEM of Flommen and previous field measurements had to use the same reference system. As the supplied DEM was based on SWEREF 99 13 30, a map coordinate transformation was necessary for conversion to SWEREF 99 TM. This was accomplished in QGIS. A stylized topographic map of Flommen, within the bounds of the coordinate system can be seen in Figure 29.

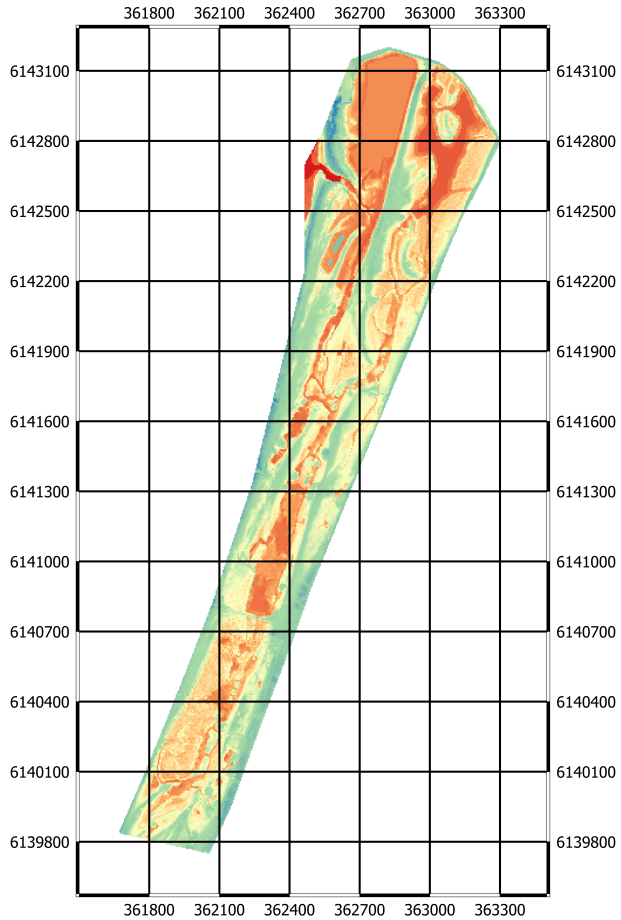

Figure 29: Image showing a stylized topographic model of the FLS. The coordinate system used is SWEREFF 99 TM. The coordinate grid resolution is 300 x 300 m.

6.1.2 Wet and Dry Effect

Due to shifting water levels in the shallow lagoon, the shape of the FLS varies over time with extent of water coverage changing regularly as seen in Figure 30. The IPH model is configured to allow for a wet and dry algorithm. Each individual cell in the mesh contains topographical data. A cell whose elevation is under the water level is considered wet, and a cell whose elevation is above the water level is considered dry. This allows the model to merge water bodies during high water levels and thus simulate a more realistic and coherent lagoon system.

Figure 30: Images showing an island in the southern part of FLS (Google Earth, 2019). The image to the left is dated 30-5-2018 and the image to the right is dated 24-02-2019. The difference in water extent is delineated by a red line on the picture to the right.

6.1.3 Grid Generation

IPH-ECO has an in-house generator for the underlying grid needed for the simulation. This generator needs a boundary file to produce the grid. The boundary file consists of the outline of the FLS, which was cropped out of a Digital Elevation Map (DEM) of the Falsterbo Peninsula, see Figure 10. Another input parameter for the grid was the resolution, which was set to 10 x 10 m. This was the highest reasonable resolution that could be used. A resolution 5 x 5 m grid could more accurately reflect the width of the canals and the lagoon system as a whole, but running a simulation on such a detailed mesh is far too time-consuming. The FLS was discretized utilizing a grid containing 17122 square elements, as seen in Figure 31.

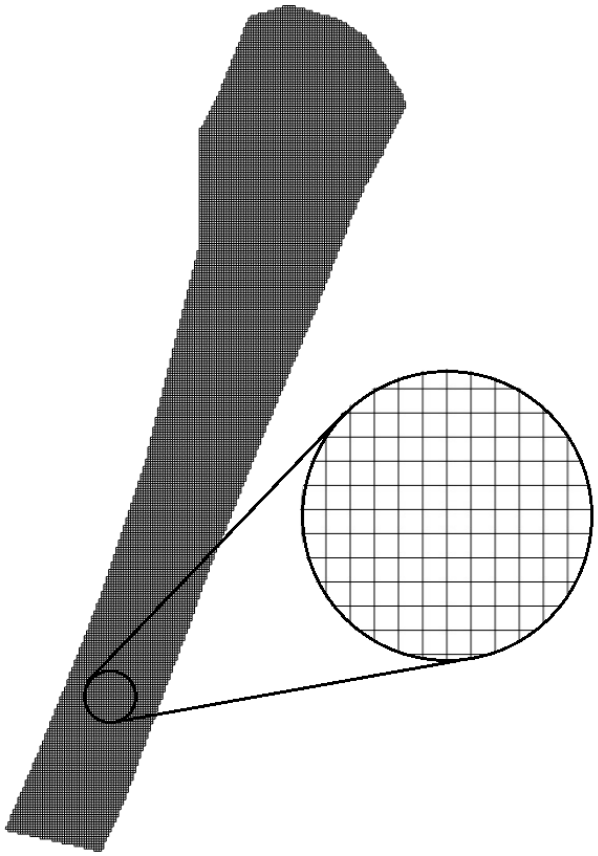

Figure 31: 10 x 10 m resolution grid generated by IPH-ECO.

6.1.4 Elevation and Bathymetry

Existing topographic and bathymetric data was used alongside on-field measurements to produce an elevation raster file of the Flommen Lagoon. The processing of the elevation raster file was completed in QGIS using bathymetry measurements collected in the field. Each point in the raster file acquired elevation data. These were then exported to a .txt file containing the coordinates and elevation of each point. The .txt file was in turn processed in IPH-ECO to apply elevation data to the mesh.

Using the .txt file, elevation data were automatically interpolated to the grid with a built-in tool within IPH-ECO. The interpolation had a radius of 20 meters. Some areas of Flommen Lagoon did not have existing bathymetric data and nor did the field measurements cover them. These areas were presumed to have similar bathymetry as the closest measured point. The final bathymetry map of FLS can be seen in Figure 32.

Due to limitations in computing power the generated mesh had a 10 x 10 m resolution. This leads to issues when attempting to simulate the flow through narrow channels whose width are smaller than 10 meters. These channels would frequently not appear in the grid after interpolation. Some of these narrow channels are crucial for a functional simulation without unreasonable model constraints. Thus, some narrow channels had to be manually manipulated to a width of 10 meters. This was done within IPH-ECO by manually changing the elevation of certain cells. Cells could be assigned a suitable elevation to allow for the flow

of water. However, this solution yields a simplification of the real geometry of the lagoon system and needs to be evaluated. This is further discussed in chapter 10.

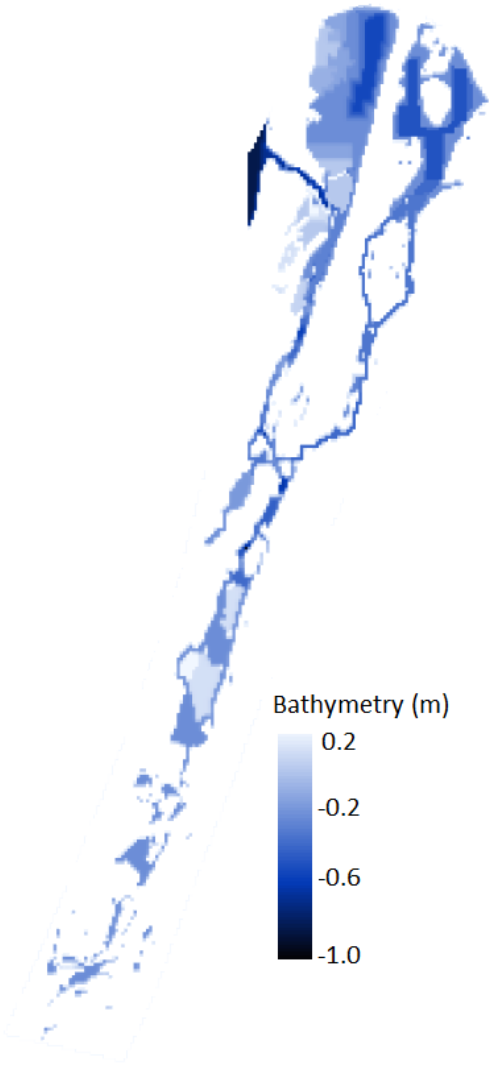

Figure 32: 10 x 10 m resolution mesh generated by IPH-ECO, with bathymetry data added. Elevations based on RH2000.

6.1.5 Roughness

Given the sandy nature of the soil combined with some organic materials, a Manning coefficient of 0.02 was assumed to apply across the whole lagoon before the calibration process. In turn, the Chèzy coefficient is calculated using equation 16, which provides a Chèzy value of 43 $m^{1/2}s^{-1}$. This equal distribution of roughness does not reflect reality, as the soil is unlikely to have exactly the same characteristics all across the lagoon. Neither is the water level constant. But due to the lack of extensive soil measurements, the assumption of a constant roughness is applied regardless.

6.1.6 Sluice Gate Representation

As mentioned in chapter 3.1, the sluice gates at the inlet provide a threshold of -0.35 m for the minimum water level and can manually be closed when the water level reaches +0.5 m. If a truly optimal model was to be attained, then this would have to be fully represented. However, IPH-ECO does not possess a tool to simulate the abrupt, but conditional blocking of water flow in Slusan that the gates is capable of.

The minimum water level threshold of the gates is applied to the model by simply assigning a bathymetry value of -0.35 m for the cells containing the gates. According to Wang (2019), the flow through the inlet has decreased since the gates was installed. Thus, it seems that the gates restricts the water flow through Slusan. In order to reflect this, a low Chèzy value is assigned to the cells representing the gates. This value is further discussed in the subsequent chapter 7.4.1.

6.1.7 Water Level Time Series

In IPH-ECO, the hydrodynamic boundary conditions for the model could be set by defining which cells should have water level variations according to the sea level outside of the lagoon. These cells were chosen manually at the boundary of the computational grid in front of the the inlet.

The water level time series are imported into IPH-ECO as a .txt file and the data is obtained from SMHI. The water level time series started two days prior to the investigated simulation period. This two-day period is defined as the spin-up time and is used to warm up the model to its full function before the simulation period of interest initiates.

6.1.8 Meteorological Data

The meteorological data inserted into IPH-ECO can influence the hydrodynamic processes. The meteorological data primarily refers to the wind, which can cause wind-induced currents. The data also contains atmospheric pressure, temperature, precipitation and evaporation. These factors can lead to currents induced by pressure gradients, but at this scale they can be considered insignificant. The wind data was obtained from SMHI with the time period of the data matching those of the water level time series. The wind data was imported into IPH-ECO as a .txt file containing the time, wind magnitude (m/s) and wind direction in terms of degrees from true north (0-360°). The atmospheric pressure was set to a constant value of 1 atm. Both air and sea temperatures were set to 20 °C. The precipitation and evaporation were set to zero, as they were deemed to have negligible impact during the relatively short simulation period in comparison with the flow between the sea and the lagoon.

6.2 Water Exchange using IPH-ECO

Tracers were applied uniformly throughout the FLS within IPH-ECO. This was done by extracting the coordinates, elevation and cell number of all cells in the grid under a certain elevation. However, since IPH has no built-in data export feature, this had to be done by using a SQL-editor to obtain and scrutinize the data from IPH to determine which cells are eligible for a tracer. Thereafter, a .txt file containing the initial cell numbers and the coordinates for the particles could be imported into IPH-ECO. This made it possible to track the movement of particles between every time step. A total of 4433 particles were deployed in the lagoon.

The analysis of flushing time and residence time is based on the tracer deployment. As described in chapter 2.3.2, the lagoon is considered flushed when the particles inside the

control region reached the lower threshold of 37%. The control region (CR), see Figure 33, is defined as the part of the lagoon being investigated for water exchange. The control section (CS) located at Slusan is the outer limit for the investigation. When the particles cross the CS the residence time is calculated. The area outside the control region enables the possibility for particles to re-enter the CR, making it possible to calculate the re-entrant residence time as discussed in chapter 2.3.3.

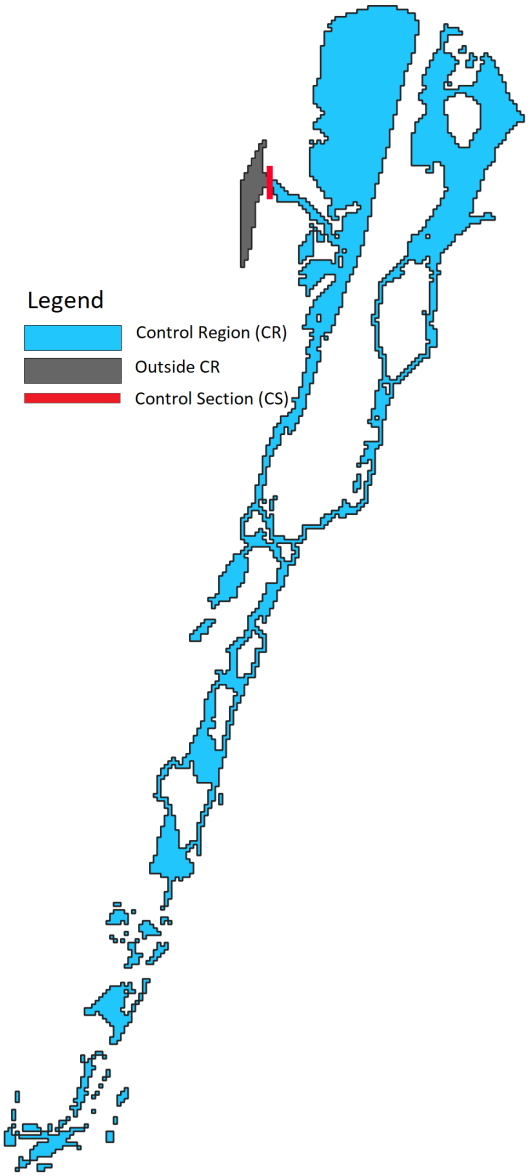

Figure 33: Grid map showing the control region (CR). Note that isolated cells can be connected to the rest of the CR through the wet and dry algorithm.

The residence time is calculated for every single particle which provides the possibility to investigate the average residence time for different parts of the FLS, as well as inspect particles

with the lowest or highest residence times.

The particle tracking is carried out based on the calibrated model during a 60-day time period. This calibrated model, with its 60-day simulation period and associated conditions is defined as the base scenario.

6.3 Model Limitations

Extracting cell information from IPH-ECO is a rather complicated process. Time and effort was required when trying to apply particles into the lagoon since the grid did not solely consist of water. Some of the tracers were inadvertently deployed to land, and some to disconnected parts of the lagoon area. These tracers had to be manually removed from the model.

There is no possibility to make the Chezy value vary depending on the water level. According to equation 16, the Chezy value is determined by the hydraulic radius and Manning coefficient. This is another source of potential error, but it is unlikely to affect the final simulation results since the variations caused by the water level are very small.

IPH-ECO is at the present unable to simulate the full effect of sluice gates. During storm events, the sluice gates are shut, blocking the flow of water through Slusan. The inability of the software to simulate this makes it less suited for modelling the effects of a storm event in the FLS.

Another possible limitation of the model is its inability to model the dynamic nature of the inlet. Sedimentation occurs with significant intensity, and the model is not able to model any possible build-up at the entry point. However, whether this would have any significant affect on the water exchange during the simulation timescale is unknown.

7 Calibration and Validation

In this chapter, the process of calibrating and validating the model is explained. Furthermore, a sensitivity analysis and a regression analysis is conducted. The result and the final parameter values used in the model following the calibration are also presented.

7.1 Calibration Process

The calibration process is a vital procedure in order to produce a viable model that consequently makes it possible to estimate the water exchange in the lagoon. A hydrodynamic calibration is accomplished by comparing a reliable data set to a similar data set produced by the model.

The water level data from the water loggers deployed in the FLS, as described in chapter 4.3, is used as the sample data. This is the data by which the model is calibrated against by comparing it to the simulated water levels at the same locations.

The calibration process is performed by adjusting parameter values affecting the simulated water level. This includes adjusting the bottom roughness and bathymetry of the lagoon. Most of the bathymetry values in the model were based on data from field measurements. However, as discussed before, bathymetric data for some parts of the lagoon are missing. This can be seen in Figure 27. This left room for some interpretations and adjustment of the data. The Chèzy coefficients were simply estimated and could repeatedly be changed during the calibration process.

Calibration was performed using the northern and southern logger as the benchmark for the first week, from the 20th of November 2019 to the middle of the 27th of November 2019 with a time step of 1 hour. This period is representative of the typical sea level fluctuations during the winter.

7.2 Validation Process

The validation process takes place after the calibration to control the quality of the calibrated model during a time period independent of the calibration time period.

For the validation, the model was run for the second week of logger deployment, from the middle of the 27th of November 2019 to the 4th of December 2019 with a time step of 1 hour. The validation is considered a success if the simulation results are deemed to fit the observed values sufficiently.

7.3 Evaluation of Model Performance

In order to evaluate model performance, estimations of the match between measured and simulated water levels are carried out. Initially, a visual estimation is done, by simply comparing the graphs and evaluating their general fit and timing of peaks. However, in order to get more distinct results, objective functions are needed.

During the calibration process, two objective functions were used; Coefficient of determination, R^2, and Root Mean Squared Error, RMSE.

7.3.1 Coefficient of Determination

The coefficient of determination, denoted R^2, is used as an output indicator during regression analysis. It is widely used as a measure of correlation between the observed data and the

data produced by the model (Nagelkerke, 1991). R^2 is defined as:

$$R^2 = 1 - [\frac{\Sigma(Q_{obs} - Q_{sim})^2}{\Sigma(Q_{obs} - Q_{obs.av})^2}] \tag{17}$$

Where Q_{obs} is the observed values, Q_{sim} the simulated values and $Q_{obs.av}$ the average value of the observed data. Should R^2 be equal to 1, 100 % of the observed values match the modelled values, i.e. it would be a perfect fit.

7.3.2 Root Mean Square Error

Root Mean Square Error (RMSE) refers to the standard deviation of the simulated values in regards to the observed values (Barnston, 1992). In this thesis, RMSE is defined as:

$$RMSE = \sqrt{[\frac{\Sigma(Q_{obs} - Q_{sim})^2}{N}]} \tag{18}$$

Where Q_{obs} is the observed values and Q_{sim} the simulated values. N refers to the sample size, which in this case is 168. This was the number of data points (corresponding to the amount of time steps) used in the calibration and validation.

7.4 Calibration and Validation Results

To see how well the simulated water level values agrees to the measured values, a linear regression plot is drawn. This is to establish if the model tends to deviate during certain water elevations.

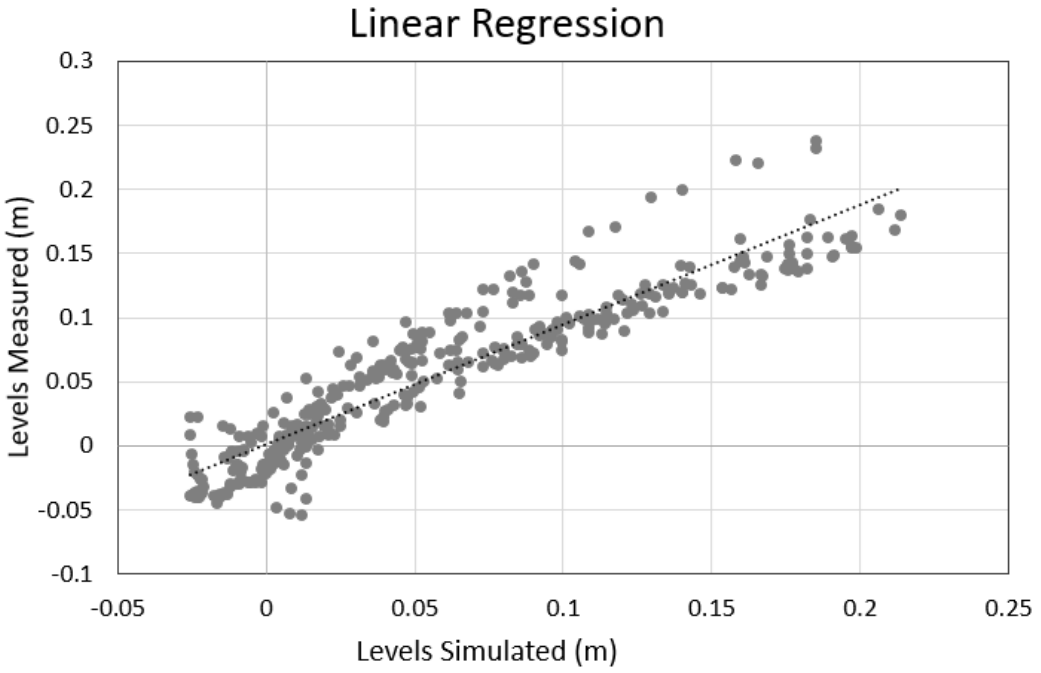

Figure 34: Linear Regression between the simulated and measured water levels. The measured water levels originated from the data set collected during two weeks by the northern logger.

As seen in Figure 34, a linear regression analysis shows how the model seems to be less accurate during peaks of high water levels but also during periods of low water elevation. This could for example be a result of the so-called hysteresis effect. When the water surface slope changes due to either rapidly rising or falling water levels in the lagoon, the hysteresis phenomenon causes the discharge to be higher during rising stages than during falling stages (Singh et al., 2011). This phenomena is not considered in the model.

However, as discussed in chapter 7.4.1 and 7.4.2, the high values of R^2 together with low RMSE-values proves that the model can reproduce the level variations in a satisfying way. Thus, the model can be trusted to simulate and portray the water exchange in FLS adequately.

7.4.1 Calibration Results

When the calibration process is complete, the model can be deemed a reasonable representation of the conditions found in the FLS. The final calibration results for the northern and the southern part of the lagoon is shown in Figure 35. Conclusive parameter values are determined by the calibration. The Chézy value is set to a constant value of 30 $m^{1/2}s^{-1}$ throughout the lagoon and thus attained a lower value than the previous estimation of 43 $m^{1/2}s^{-1}$ as described in chapter 6.1.5. In areas of the lagoon where bathymetry data was missing, adjustments could be performed liberally in order to improve the model. The bathymetry in Slusan is set to -0.6 m. To simulate the choked inlet flow caused by the sluice gates, the cells containing the gates was given a bathymetry value of -0.35 m and a calibrated Chézy value of 1 $m^{1/2}s^{-1}$.

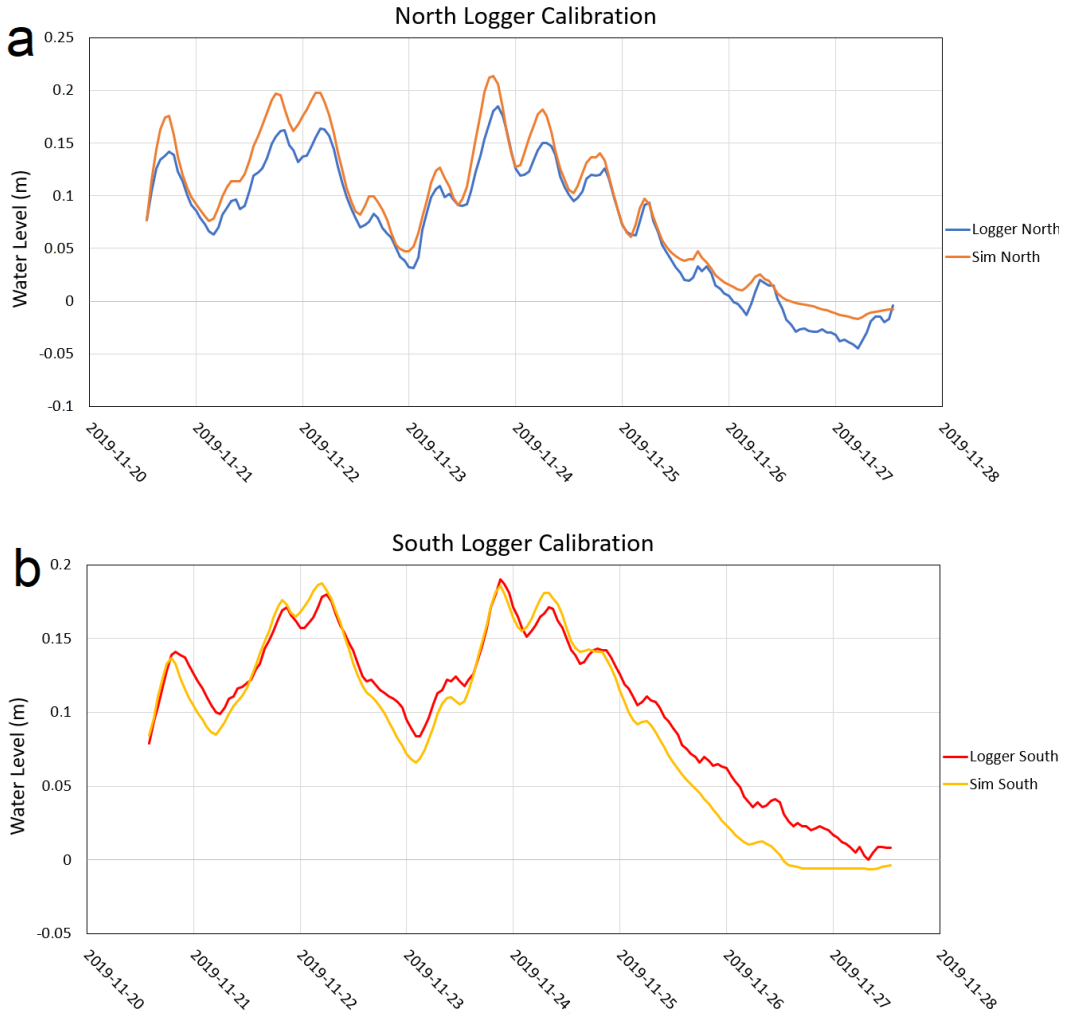

Figure 35: Graphs showing the correlation between the final calibrated simulation and the measured data from the northern logger and the southern logger.

The R^2 and Root Mean Square Error (RMSE) for the calibration simulation of the northern part of FLS, displayed in Figure 35a, were calculated to be 0.971 and 0.0201 m respectively.

The calibration of the southern part of the lagoon seen in Figure 35b, resulted in a R^2 of 0.9765 and a RMSE of 0.0174 m.

7.4.2 Validation Results

To verify the performance of the model, a validation was performed. The result of the validation is shown in Figure 36.

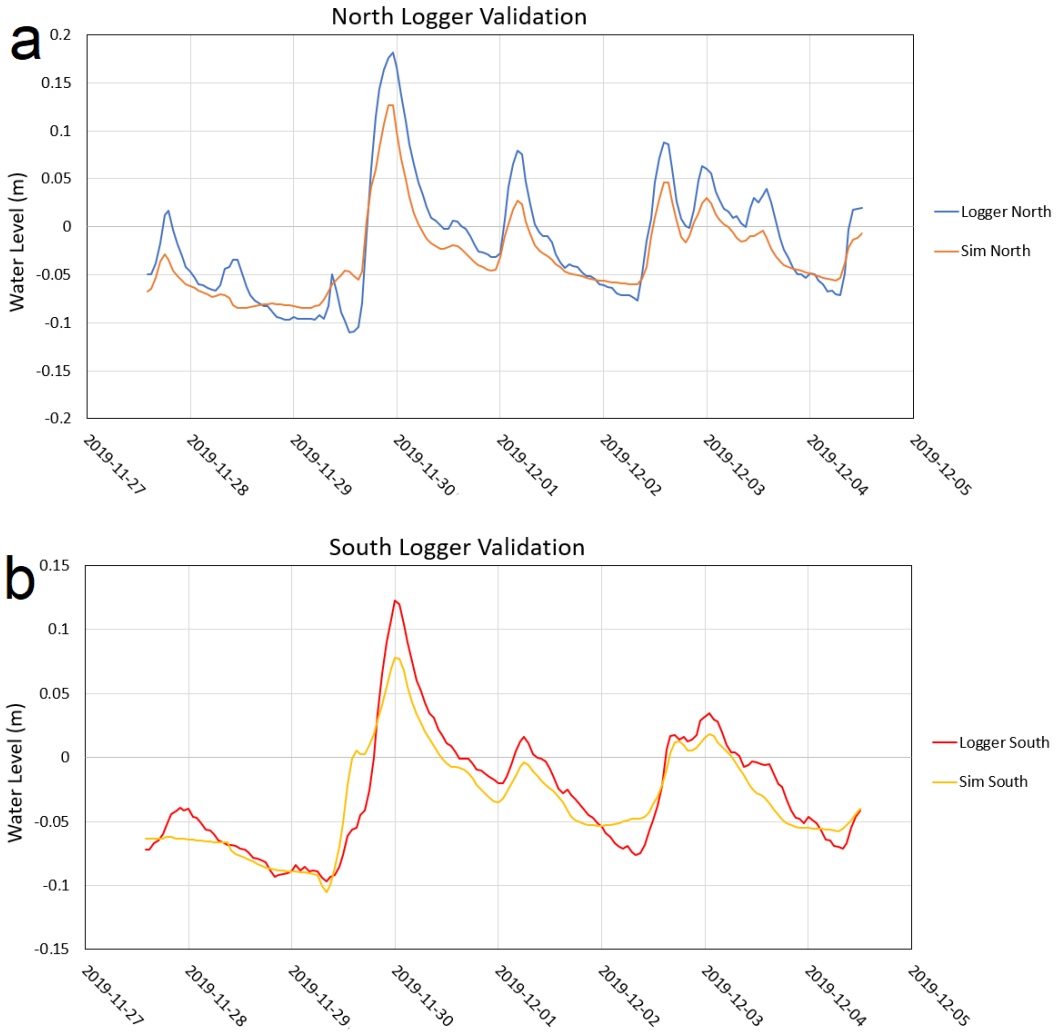

Figure 36: Graph showing the water level from the validation simulation and its correlation with the data from the northern and the southern logger.

The validation of the northern part of FLS, see Figure 36a, resulted in a R^2 of 0.911 and a RMSE of 0.027m. This is a similar result as the result from the calibration, which validates the pleasing performance of the model.

The R^2 and RMSE for the validation simulation of the southern part of FLS seen in Figure 36b, were calculated to be 0.881 and 0.0282m respectively.

The validation verifies the results from the calibration and the final parameter values used in the model.

7.5 Sensitivity Analysis

A sensitivity analysis was conducted to estimate the effect of different parameter values within the simulation. The parameter values tested were the Chèzy values of the cells representing

the sluice gates, the intensity of the wind and the Chèzy value representing the bottom roughness of the whole lagoon. These parameters were selected for analysis due to their assumed impact on the water exchange in the lagoon. Conducting a sensitivity analysis on the bathymetry of the lagoon would have been too comprehensive and time-consuming.

An increase and a decrease, in regards to the calibrated base value was respectively applied to each of the parameters.

During the sensitivity analysis the base value of the wind intensity was set to the most common value of 6 m/s, with a wind direction from south west (240°), since this one of the predominant directions.

Each parameter was analysed separately. For example, a high-end value was assigned to the Chèzy cells representing the gates and then a simulation was run. After the said simulation was complete, a low-end value was assigned to the same cells and another simulation was run. Thereafter, the output from the simulations were compared with the output from the calibrated model by evaluating the Root Mean Squared Error(RMSE).

For each run, only one parameter was assigned their test value, with the other parameters retaining their base values.

Table 1: Table showing the different parameters, their values and the associated Root Mean Square Errors (RMSE) between their resulting output and the output from the base values.

	Whole Lagoon Chézy Value ($m^{1/2}s^{-1}$) *Base Parameter Value= 30*	
Parameter Value	15	60
RMSE (m)	0.0063	0.0021

	Sluice Gate Chézy Value ($m^{1/2}s^{-1}$) *Base Parameter Value= 1*	
Parameter Value	0.5	2
RMSE (m)	0.0008	0.0007

	Wind from South West (m/s) *Base Parameter Value= 6*	
Parameter Value	0	12
RMSE (m)	0.0112	0.0033

It should be noted that the simulations run during the sensitivity analysis were merely one day long with a spin-up time of two days. The main purpose of the analysis is to show the effect that each individual parameter has on the model when they have high and low values respectively.

As seen in Table 1, decreasing the Chèzy value in the whole lagoon from 30 $m^{1/2}s^{-1}$ to 15 $m^{1/2}s^{-1}$, produces a RMSE of 0.0063m between the outputs. However, when increasing the Chèzy value to 60 $m^{1/2}s^{-1}$ the RMSE is 0.0021. This suggests that the model is more sensitive for low Chèzy values in the whole lagoon.

The cells representing the sluice gates had very small Chèzy values in order to portray the present situation at Slusan. The base value of 1 $m^{1/2}s^{-1}$ seems to have very similar outputs as the simulations with a Chèzy value of 0.5 and 2 $m^{1/2}s^{-1}$, resulting in a RMSE of 0.0008m and 0.0007m respectively.

The wind speed seems to have a significant impact on the simulation result. The output from the simulation with no wind seems to deviate more from the base value compared to the one

with a wind speed of 12 m/s, with a RMSE of 0.0112m and 0.0033m respectively.

8 Simulation Results

8.1 Flushing Time

The flushing time of the lagoon is defined in equation 4. The results from the simulation, consisting of tracers and their movement throughout the simulation period, were processed using MATLAB. The simulation period spanned between January 5th to March 6th 2019, a total of 60 days. The wind and water level data for this period is retrieved from SMHI. This period is chosen as it is considered to be representative of the prevailing conditions usually found in the area. The tracers were released during a rise in sea water level outside of the lagoon leading to an inflow of particles to the CR during the initial time steps.

This simulation, with its associated conditions and period, is considered the base scenario.

The results are presented in the Figure 37.

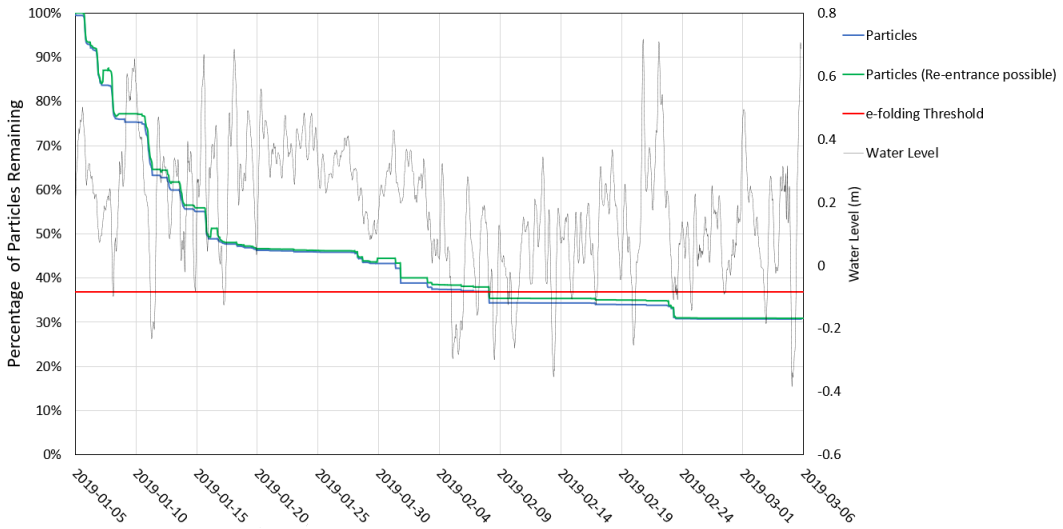

Figure 37: Figure showing the decrease in average tracer concentration (%), for 60 days. The blue line represents the decrease in particles without re-entry to the control region. The green line represents decrease in particles with the possibility for re-entry. Additionally, the water level input is also plotted.

The calculated flushing time was roughly 33 days, as the particle line crosses the e-folding threshold at this time. The calculated flushing time with re-entrance allowed showed a tiny difference compared to the flushing time with re-entrance disabled. A sharp decrease of particles within the lagoon during the first 12 days when the sea water level is decreasing and the water is flowing out of the FLS, can be observed. During the first 12 days, the particle concentration in the lagoon decreases from 100% to 53%. After these 12 days the particle lines starts to flatten out, signaling a slower particle decrease. This can possibly be explained by the fact that, during the first 12 days, a lot of particles in the vicinity of Slusan, including the northwestern part, exits the FLS. Thenceforth, particles deeper within the lagoon takes a longer time to exit the CR. Some particles might also get stuck inside the lagoon.

8.2 Residence Time

The concept of residence time is explained in chapter 2.3.3. The results from the simulation, consisting of tracers and their movement throughout the simulation period, were processed using MATLAB. Further processing of the data was conducted in QGIS. The end-result was essentially a interpolated particle map showing the residence time of each individual tracer. The map, as seen in Figure 38, shows noticeable differences in residence time between different parts of the lagoon.

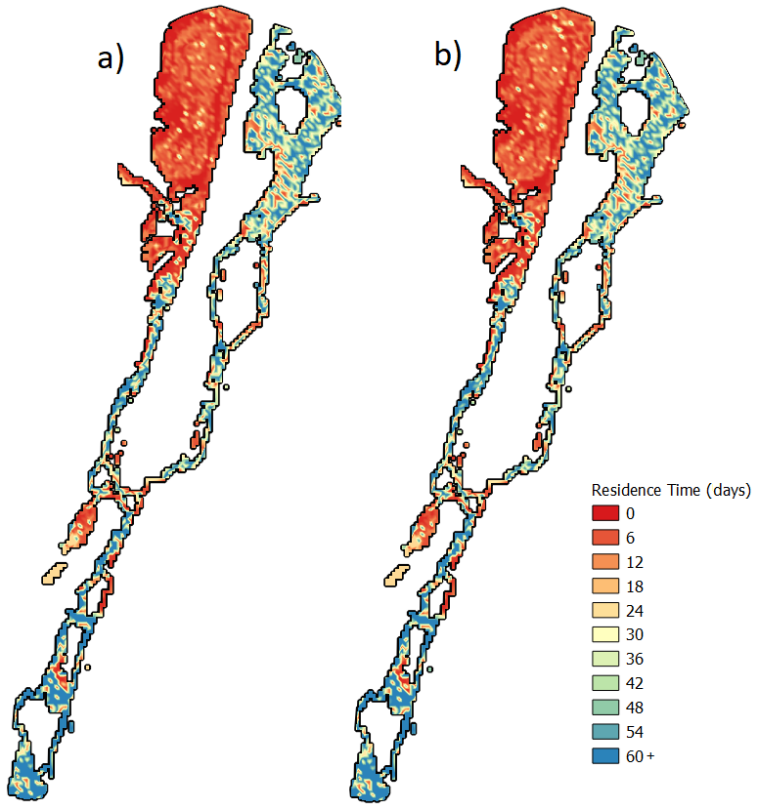

Figure 38: Map showing simulated residence time in the control region of Flommen Lagoon system. a) is the result without any particle re-entry. b) is showing re-entrant residence times.

Table 2: Table of the difference between the normal residence time and the re-entrant residence time for the whole lagoon. The maximum, minimum and average residence time for all the particles is presented.

	Flommen Lagoon System (Whole Lagoon)	
	Residence Time	*Re-entrant Residence Time*
Max Value	+60 days	+60 days
Min Value	18 hours	18 hours
Average Value	26 days & 21 hours	27 days & 6 hours

The average residence time for all the particles in the lagoon is almost 27 days as seen in Table 2. The difference in re-entrant and once-through residence time is negligible. This could be due to the limitations of the model. The control section is barely two cell rows away from the exit line. This leaves particles with little chance to re-enter the CR. The shortest time a particle spends in the system is 18 hours after the release of particles.

Investigations of local residence times in different parts of the lagoon were conducted to get a clearer view of the most fragile parts of the lagoon in terms of water quality. The northwestern, northeastern and the southern part of FLS, seen in Figure 39, were examined.

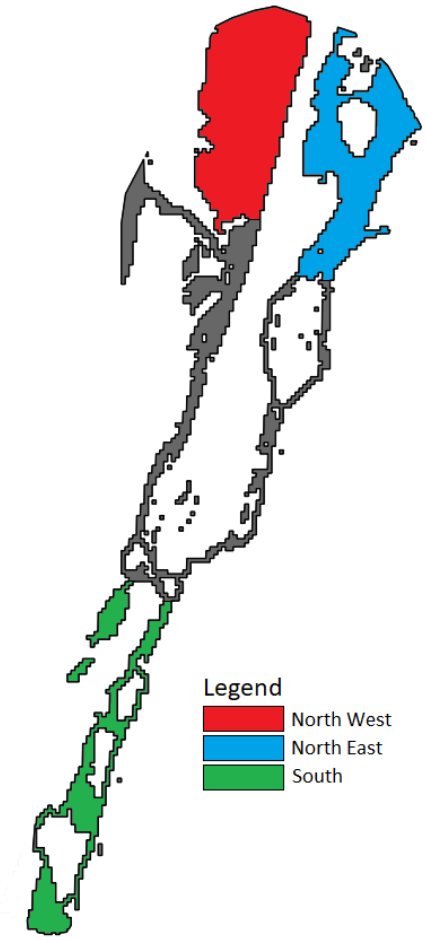

Figure 39: Different parts of the lagoon which have been evaluated for separate residence times.

Table 3: Table of the difference between the normal residence time and the re-entrant residence time for different parts of the FLS. The maximum, minimum and average residence time for all the particles is presented.

a)	**Northwest**	
	Residence Time	*Re-entrant Residence Time*
Max Value	49 days	+60 days
Min Value	18 hours	18 hours
Average Value	6 days	6 days & 7 hours

b)	**Northeast**	
	Residence Time	*Re-entrant Residence Time*
Max Value	+60 days	+60 days
Min Value	2 days	2 days & 14 hours
Average Value	40 days & 14 hours	41 days

c)	**South**	
	Residence Time	*Re-entrant Residence Time*
Max Value	+60 days	+60 days
Min Value	2 days	2 days
Average Value	42 days & 18 hours	43 days

As shown in Tables 3a-c and Figure 38, the average residence time for different parts of the lagoon differs greatly. As expected, the northwestern part of the lagoon has an extremely low residence time. The minimum residence time of 18 hours in the northwestern part, see Table 3a, equals the minimum residence time for the whole lagoon shown in Table 2. Its average value of 6 days stands in contrast with the average +40 days residence time found in the south and northeastern parts of the lagoon as seen in Table 3b-c. Two days after the release of particles, the first particles from northeastern and southern parts of the FLS leave the lagoon. However, the majority of particles in these areas reside in the lagoon for a longer time, possibly indicating water quality issues. The reason for these differences is likely the proximity of the inlet Slusan. The northwestern part of the lagoon is vastly closer to Slusan. Particles dropped over that part of the lagoon have a comparatively shorter distance to travel in order to leave the CR when there is an outflow. Particles originating deeper inside the lagoon not only have a longer distance to travel, but they also have a higher risk of getting stuck due to the wet and dry algorithm. An example of a stuck particle is shown in Figure 40a.

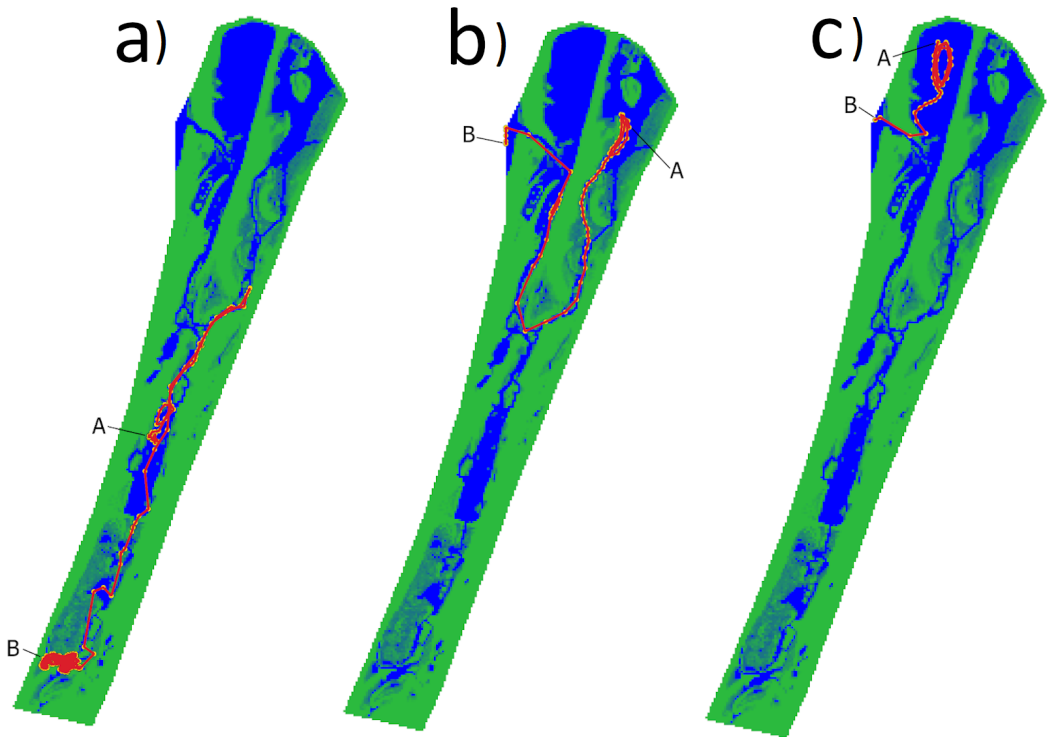

Figure 40: Sample pictures of particle movement in the simulation results. A denotes the starting position, B denotes the final position. Figures 40a-40c shows particles starting in the southern, northeastern and northwestern part of the lagoon respectively. Note that Figure 40a shows an example of a particle ending up stuck in the southernmost part of the lagoon.

8.3 Velocity Fields

For a more visual perception of the flow patterns and the velocities in different areas of the FLS, velocity field maps were produced. Figures 41 and 42 show largest velocities at the inlet and in the narrow channels south of the inlet.

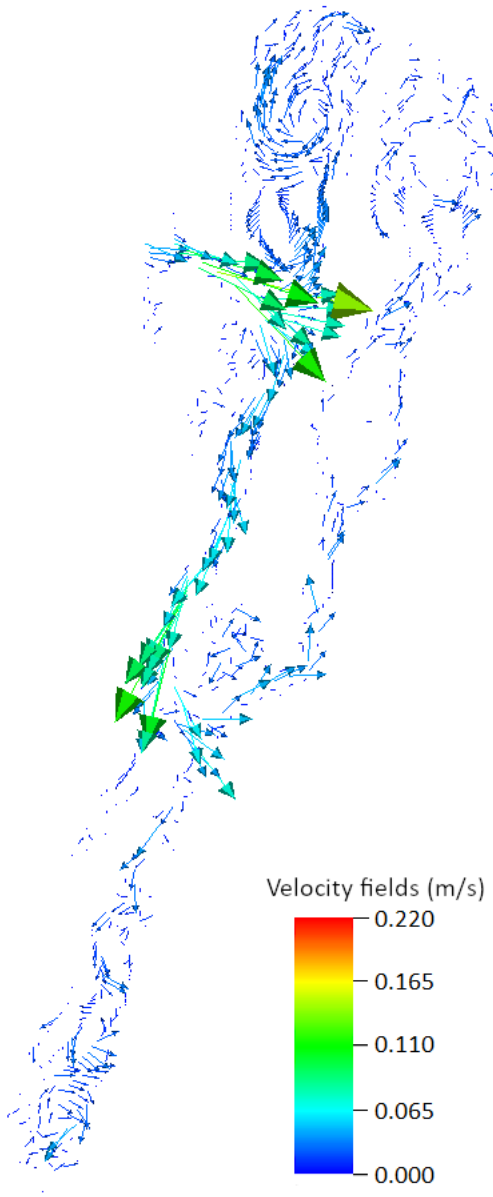

Figure 41: Simulated velocity fields in the lagoon during the time step with the highest inflow.

During a high inflow, see Figure 41, the highest simulated velocity was found at Slusan, and measured roughly 0.14 m/s. The narrow channel south of the inlet sees velocities of around 0.11 m/s. In the southern and northeastern parts the velocities are very low and the velocity vectors might be mostly wind induced, probably resulting in low local mixing.

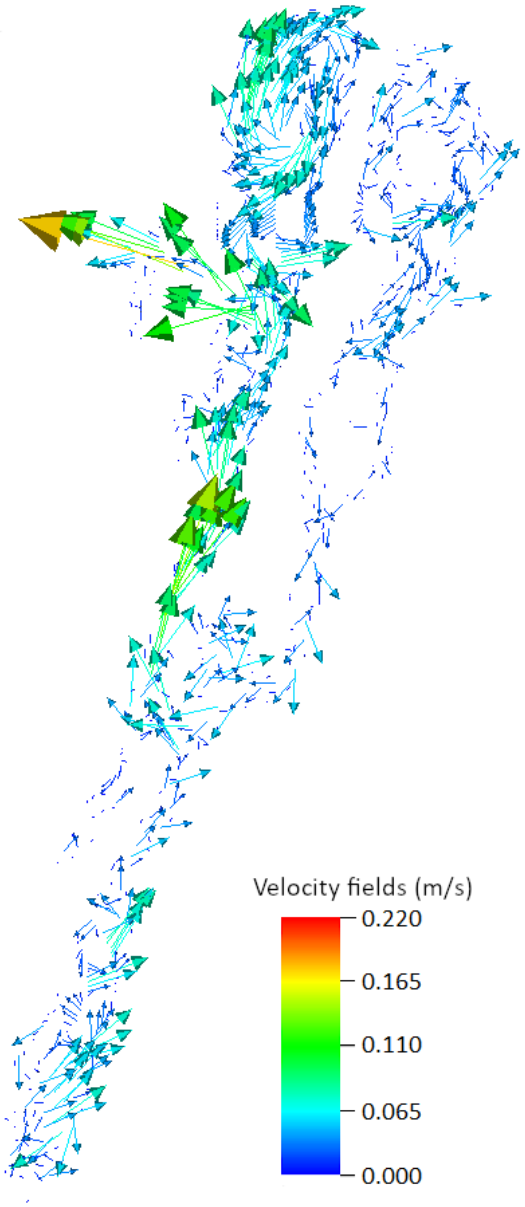

Figure 42: Simulated velocity fields in the lagoon during the time step with the highest outflow.

During a high outflow, see Figure 42, the highest simulated velocity was found at Slusan, and measured roughly 0.18 m/s which slightly higher than the maximum velocity during inflow. It also seems like the velocities are marginally higher deep within the lagoon during outflow.

The velocity fields, as visualised in Figures 41 and 42, showcases the typical behavior exhibited by the flows inside the lagoon during high inflow and outflow. Velocities reach relatively high levels compared to the rest of the lagoon near Slusan. Velocities tend to decrease deeper inside the lagoon. In the north eastern and southern parts of the lagoon, the circular movement of the velocity vectors seems to suggest that they are mostly influenced not by tidal force, but

by the wind. This further explains the relatively high residence time found in these areas.

Even though the velocities are relatively high near Slusan with a maximum outflow velocity of 0.18 m/s, they are not strong enough to prevent issues with the sedimentation near the inlet, caused by longshore sediment transport as discussed in chapter 3.2.

9 Different Simulation Scenarios and Their Results

In this section, several scenarios concerning the layout of the lagoon are discussed and presented. Their effects on the water exchange are also elaborated on. These scenarios are sinusoidal sea level variations, a new inlet constructed whilst Slusan remains open and a new inlet constructed with Slusan closed.

9.1 Sinusoidal Sea Level Variation

Two sinusoidal sea level scenarios were simulated. These sinusoidal sea level variations have an amplitude of 0.5 m and 0.1 m respectively with the baseline at 0 m. Both variations have a period of 1 day, and both scenarios were run for 60 days. The simulations were performed without wind forcing and the tracers were released during inflow to the lagoon.

This study was conducted in order to get a more throughout conception on how the amplitude of the sea water level is affecting the water exchange in the lagoon.

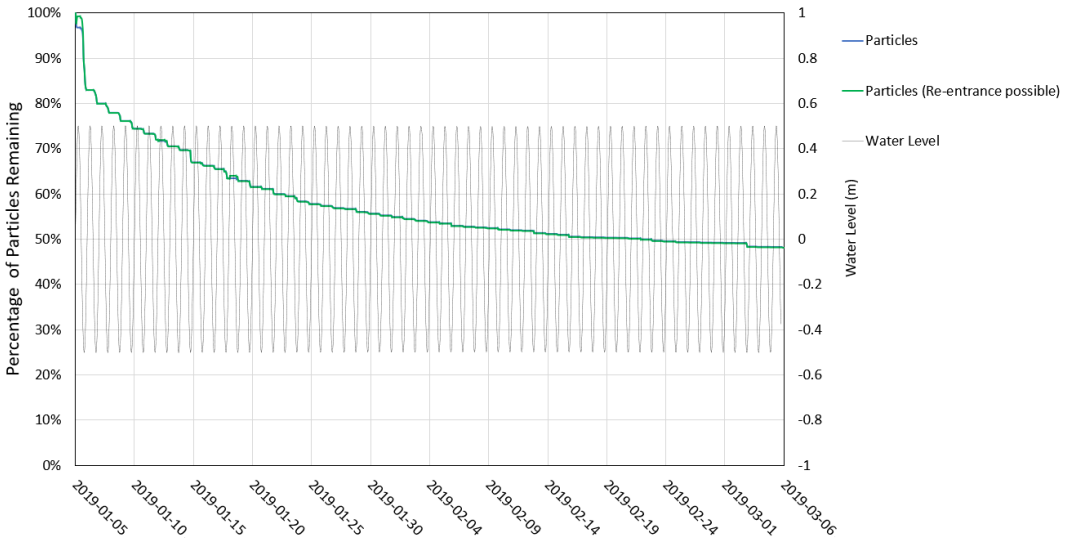

Figure 43: Graph showing the sine water level variation with an amplitude of 0.5 m and its effect on the particle flushing. Results for both with and without particle re-entrance are shown.

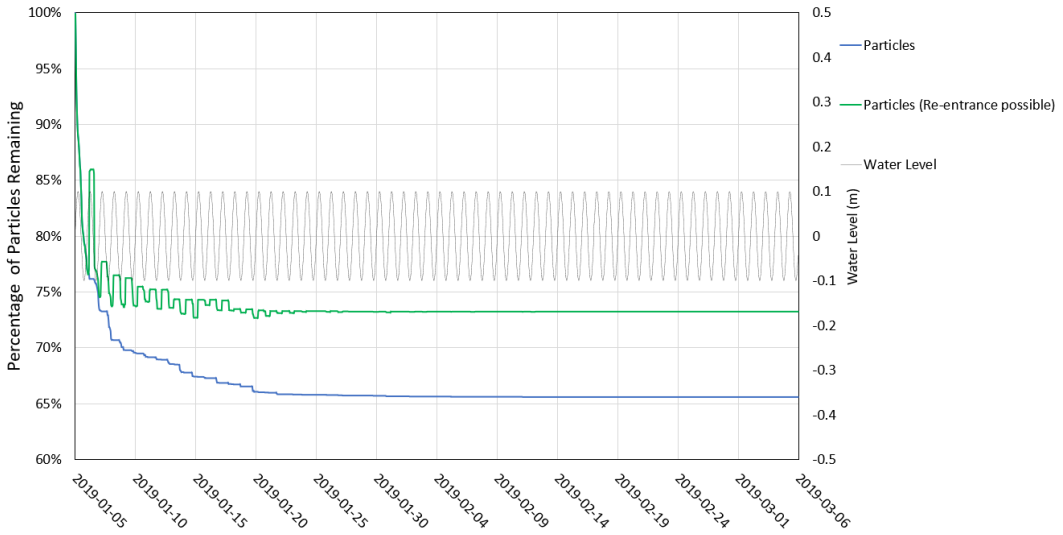

Figure 44: Graph showing the sine water level variation with an amplitude of 0.1 m and its effect on the particle flushing. Results for both with and without particle re-entrance are shown.

Note the differences in flushing between the two sine sea level scenarios. The sine sea level variation with a 0.5 m amplitude in Figure 43, seems to steadily flush out particles. Even though the rate of particle flushing seems to be declining, it remains existent for a longer period than the 0.1 m amplitude scenario, seen in Figure 44. However, even if the simulation were to continue for a few more months, it is very unlikely that the e-folding threshold of 37% would be reached. This might be a result of the particles deep within FLS not reaching the CS before they get flushed in again. The simulated sinusoidal scenario with an amplitude of 0.5 m seems to be flushing out around 51% of the particles in 60 days. It can be noted that allowing particle re-entry seems to have negligible effects on the flushing time. This can possibly be explained by the approximate 12 hour duration of the outflow and inflow to the lagoon. This, combined with the relatively high amplitude, causes the particles leaving the control section to also leave the exit boundary of the grid before having the possibility to change direction and return to the lagoon.

The simulation of sine water level variation with an amplitude of 0.1 m showcases a lower water exchange capability compared to the 0.5 m amplitude scenario. After a brief window of particles exiting, the rate of particles leaving the lagoon essentially flatlines. For the non re-entrant particles and re-entrant particles released in the CR, only around 34% and 27% of the particles are flushed out respectively.

The two sine water level variation scenarios show that the sea level amplitude variations have a big impact on the magnitude of water exchange in the lagoon. However, the scenario with a relatively large water level variation with an amplitude of 0.5 m, never reached the e-folding threshold. This stands in contrast with the base simulation, as discussed in chapter 8.1, that had a resulting flushing time of 33 days.

The reasons why the results in the sine variation scenarios never seem to reach the e-folding threshold might be due to several reasons. One of these could be the lack of wind influence in the simulation. Another one could be the limited time periods where the outflow occurs. If compared with the base results in chapter 8.1, it seems that a sustained outflow during a

longer time period is more conductive for a shorter flushing time. One other possible factor influencing the results is the sluice gates during low sea levels.

9.2 New Inlet

In a report issued by the Danish Hydrological Institute (2018), one of the suggested solutions to maintain the water exchange in Flommen is establishment of a new inlet directly north of the harbour. The low morphological activity of this area is of vital importance to the new inlet, as it diminishes the problem of sedimentation and minimises the impacts on the coastline. However further investigations of the sediment transport in this area are required in order to rely on this solution.

One or two jetties could help stabilise the inlet and prevent the occurrence of sedimentation problems as well. This inlet will be connected to Flommen through a new canal under the Skanör Harbour road. One possibility could be to let the water flow through a culvert. Figure 45 shows the location of the proposed canal and new inlet.

Figure 45: Suggested inlet north of the harbour. Yellow lines signify the proposed jetties. Blue lines under the Skanör Harbour Road signifies the new canal. The red lines indicate the 2007 coastline (Danish Hydrological Institute, 2018).

The impact on the water exchange in Flommen that this solution would have is so far unknown. Due to the model boundaries, which does not extend north of the Skanör Marina road, only the canal under the Skanör Marina road can be simulated. For the sake of this simulation, it is assumed that the construction underneath the road will be a culvert. In the model, this will be represented by a body of water replacing what was previously land. A water level time series matching those of the standard scenario is implemented in the most northernmost cells of the culvert. The roughness of this new canal is assumed to be slightly lower than the lagoon itself, with a Chézy value of 50 $m^{1/2}s^{-1}$ representing a smoother surface. The width of this new inlet is set to 10 m, equal to one cell.

Two different new inlet scenarios are investigated. One scenario with both Slusan and the

new inlet open and one scenario only with the new inlet open. Figure 46 shows how the scenario with both inlets open looks like inside IPH-ECO.

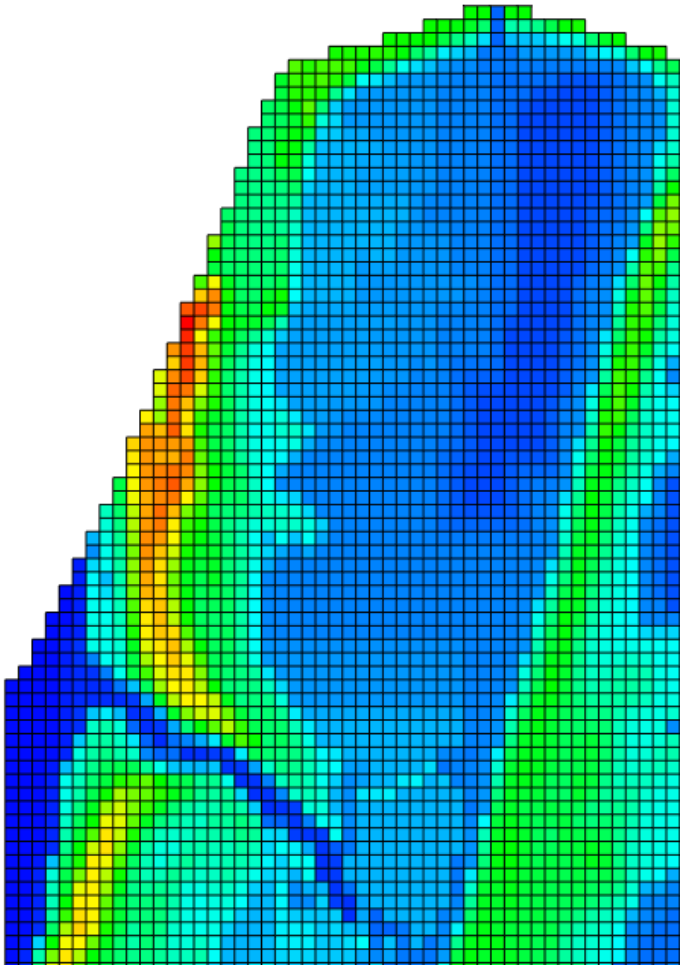

Figure 46: Proposed new inlet as simulated inside the model.

9.3 Results - New Inlet

The result in this section is based on the scenario with both Slusan and the new inlet open.

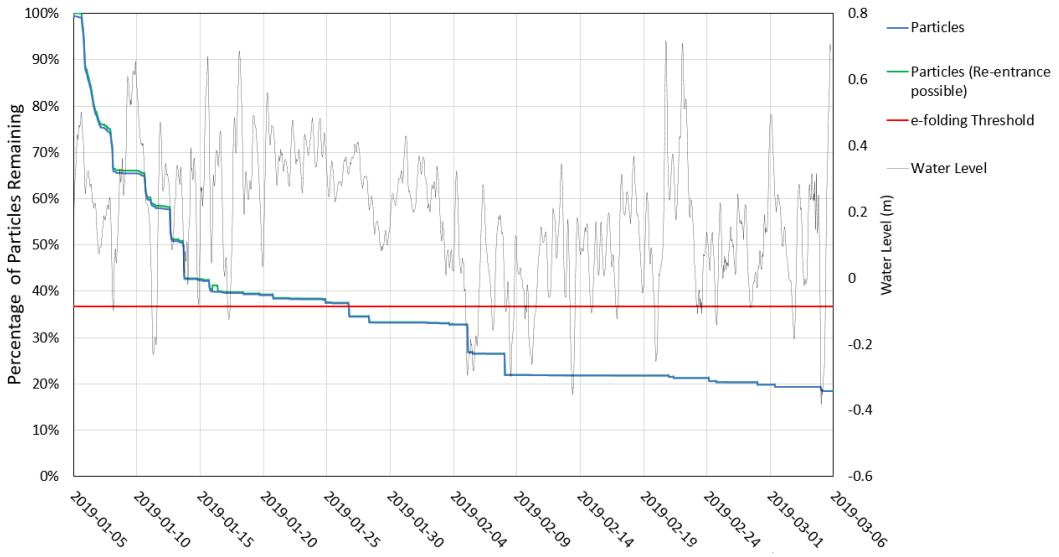

Figure 47: New inlet scenario with Slusan open. Figure showing the decrease in average tracer concentration (%), for 60 days. The blue line represents the decrease in particles without possibility for re-entry to the control region. The green line represents decrease in particles with the possibility for re-entry. Additionally, the water level input is also plotted.

The simulated e-folding flushing time for the new inlet scenario with Slusan open, as seen in Figure 47, is roughly 22 days. This is a decrease of the flushing time with 11 days compared to the current situation without a new inlet.

The construction of a new inlet seems to reduce the flushing time in the lagoon and improve the water quality. In reality, due to sedimentation issues, it is unlikely that Slusan would remain open unless additional dredging efforts are put into place.

Like the base scenario, allowing re-entry leads to negligible differences in flushing time.

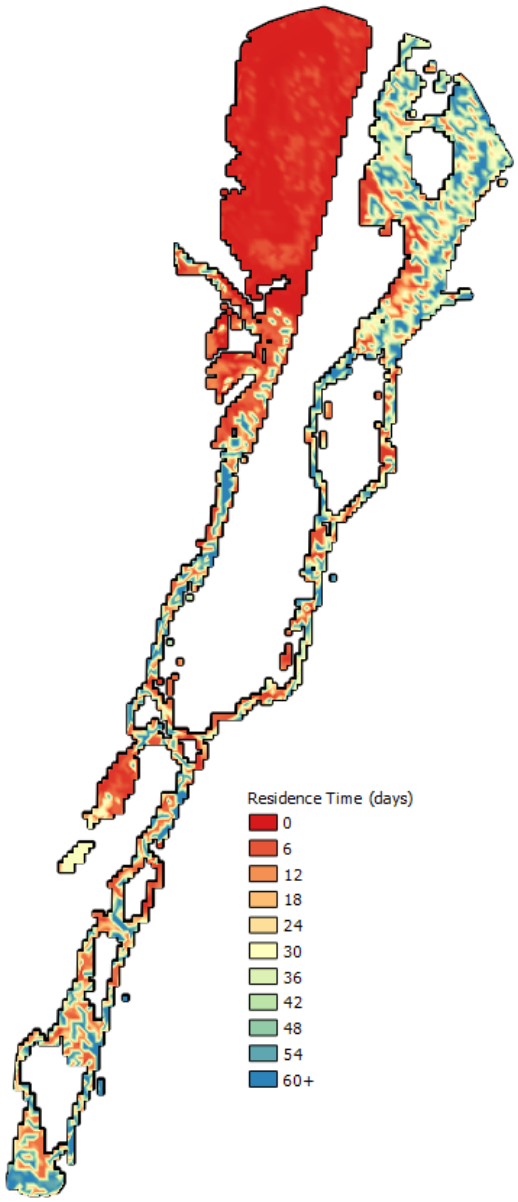

Figure 48: Simulated residence time in the new inlet scenario with Slusan open.

The reduction in residence time, as seen in Figure 48 is not confined solely to the northwestern part of the lagoon closest to the inlet. If compared with the base scenario (Figure 38), it seems that the southern and northwestern parts of the lagoon also see noticeable reductions in their residence time.

The average residence time was calculated to be 21 days as seen in Table 4a.

Table 4: Table of the difference between the normal residence time and the re-entrant residence time for different parts of the lagoon. The maximum, minimum and average residence time for all the particles is presented. New inlet scenario with Slusan open.

a)	**Flommen Lagoon System (Whole Lagoon)**	
	Residence Time	*Re-entrant Residence Time*
Max Value	+60 days	+60 days
Min Value	15 hours	15 hours
Average Value	21 days	21 days

b)	**Northwest**	
	Residence Time	*Re-entrant Residence Time*
Max Value	9 days	9 days
Min Value	15 hours	15 hours
Average Value	2 days	2 days

c)	**Northeast**	
	Residence Time	*Re-entrant Residence Time*
Max Value	+60 days	+60 days
Min Value	3 days	3 days
Average Value	35 days	35 days

d)	**South**	
	Residence Time	*Re-entrant Residence Time*
Max Value	+60 days	+60 days
Min Value	2 days	2 days
Average Value	30 days	30 days

The results in Tables 4a-d, reinforce the previous results as seen in Figure 48. The northwestern part of FLS has the shortest residence times with an average of 2 days. This is 4 days less than the base scenario without the new inlet. The northeastern part of the lagoon had the worst water exchange in the lagoon, with an average residence time of 35 days (Table 4c). However, this is 5 days less than the base scenario. There is no significant difference between the once-through and the re-entrant residence time for the new inlet scenario.

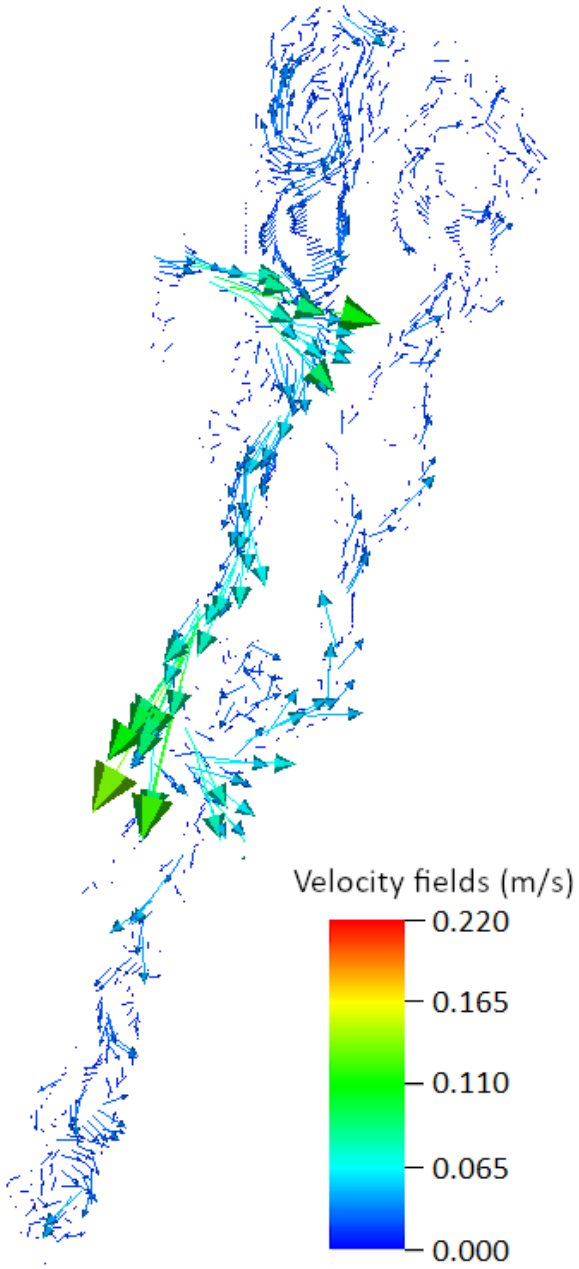

Figure 49: Simulated velocity fields in the lagoon during the time step with the highest inflow.

Unsurprisingly, the velocity fields during high inflow attain their highest values near Slusan and the channel directly adjacent south of Slusan. This can be seen in Figure 49. Velocity fields in the rest of the lagoon seem to be dominated by wind-induced forces, given their circular patterns.

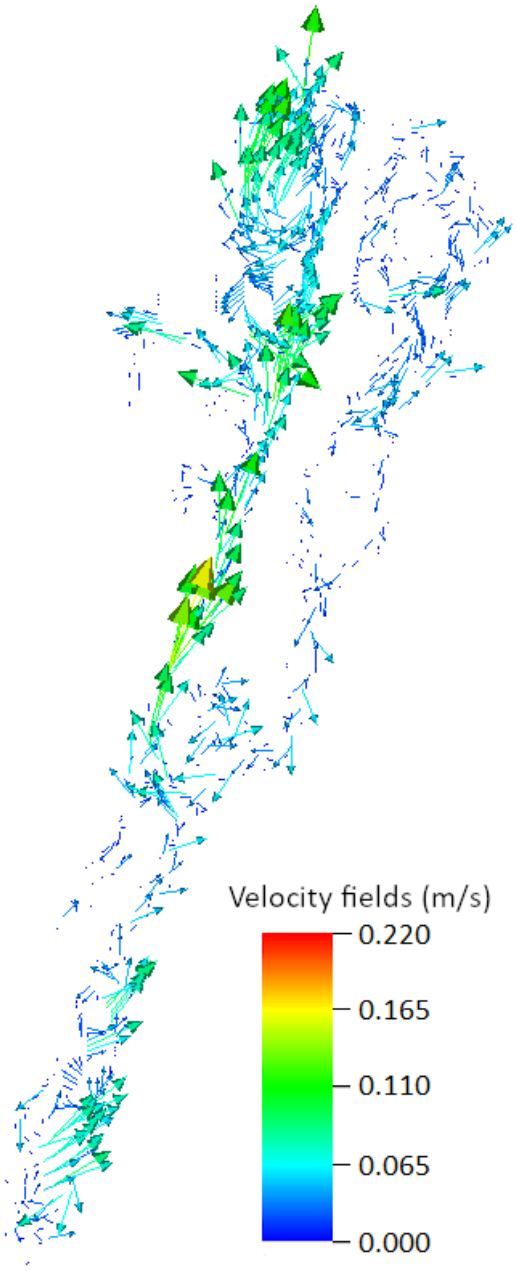

Figure 50: Simulated velocity fields in the lagoon during the time step with the highest outflow.

Gauging the velocity fields across the whole simulation period leads to some interesting observations. Both the ingoing and outgoing velocity through Slusan seems to decrease due to the new inlet. As seen in Figures 49 and 50, the ingoing velocity is approximately 0.11 m/s and the outgoing velocity is around 0.08 m/s, compared to 0.14 m/s and 0.18 m/s without the new inlet during the same timestep (see Figure 41 and Figure 42).

Given the already excessive issues with sedimentation at Slusan, it seems the construction

of a new inlet will only further exacerbate the problem. More simulations should be done to investigate this.

9.4 Results - New Inlet with Slusan closed

The results presented in this section is based on the scenario where Slusan is closed and the new inlet is open. The e-folding flushing time for this scenario is more than 60 days as seen in Figure 51. After 60 days around 41 % of the particles remain in the lagoon.

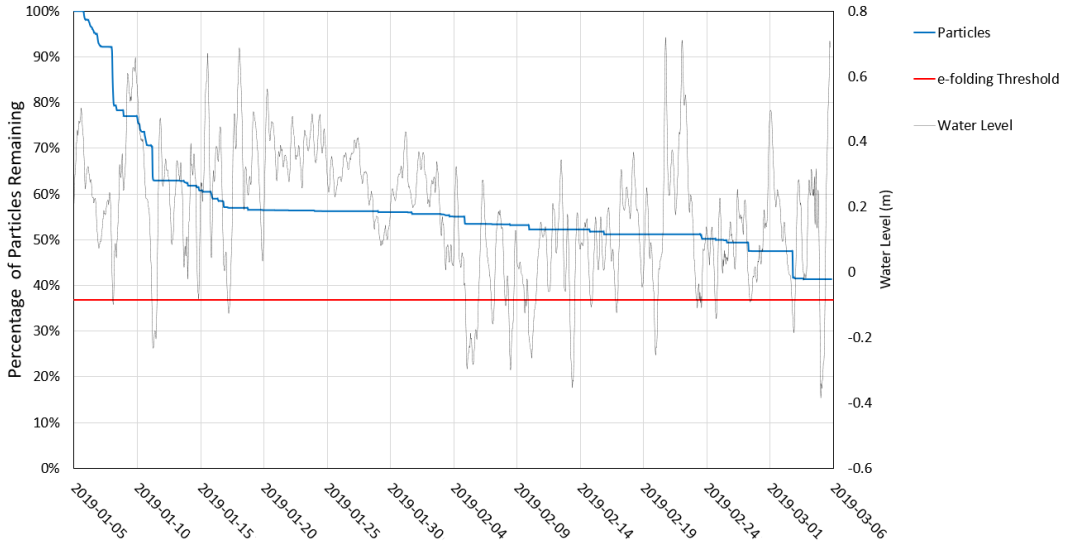

Figure 51: New inlet scenario with Slusan closed. Figure showing the decrease in average tracer concentration (%), for 60 days. The blue line represents the decrease in particles without possibility for re-entry to the control region. Additionally, the water level input is also plotted.

The variance of residence time in the FLS is illuminated in Figure 52. It shows a significant difference between areas far away from the new inlet, with large residence times, compared to areas in vicinity to the new inlet.

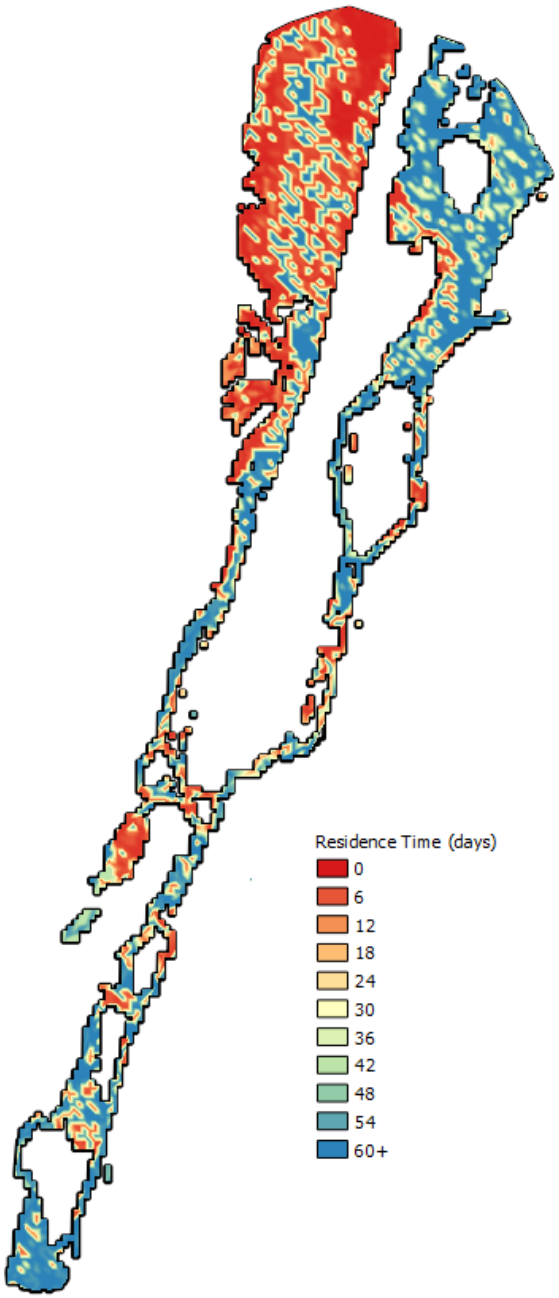

Figure 52: Simulated residence time in the new inlet scenario with Slusan closed.

The residence time varies between 18 hours to 60+ days and the average residence time for the whole lagoon is 34 days, see Table 5a. This is almost 8 days more than the average residence time calculated in the base scenario. The average residence time for the northwestern part of the FLS, shown in table 5b, adjacent to the new inlet had the lowest value of 18 days. The part of the FLS with the worst water exchange is the northeastern part with an average residence time of 47 days, compared to the base scenario with an average residence time of almost 41 days.

Table 5: Table of the difference between the residence time for the FLS and different parts of the FLS. The maximum, minimum and average residence time for all the particles is presented. New inlet scenario with Slusan closed.

a)	**Flommen Lagoon System (Whole Lagoon)**
	Residence Time
Max Value	+60 days
Min Value	18 hours
Average Value	34 days

b)	**Northwest**
	Residence Time
Max Value	+60 days
Min Value	18 hours
Average Value	18 days

c)	**Northeast**
	Residence Time
Max Value	+60 days
Min Value	3 days
Average Value	47 days

d)	**South**
	Residence Time
Max Value	+60 days
Min Value	3 days
Average Value	43 days

10 Discussion

IPH-ECO, with its versatility and processing abilities, made it possible to model and simulate the hitherto unknown water exchange in the FLS. The measurements conducted in the field, in conjunction with the field measurements by Wang (2019) aided in a satisfactory calibration. The results have deemed reliable, paving the way for further investigations on the lagoon in the future.

However, it should be stressed that this model is not reality but merely a simplification of reality. Reality is too complex to model completely faithfully and a fine line between complexity and accuracy should be the goal. Hence, the results from this thesis should not be interpreted as the absolute truth, but as an reasonable estimation.

Given the fact that the model was calibrated and validated using data during winter, it should be expected that the model is more accurate for this season. Climate change is also bound to affect the sea level fluctuations, thus affecting the accuracy of the model in the future.

The water exchange is diminished by closing Slusan and building a new inlet in the north. Sedimentation issues at this new inlet should be considerably less than those currently experienced in Slusan, leading to less frequent dredging and reducing costs according to Danish Hydrological Institute (2018). However, it should be noted that the reduction of costs could come at the expense of a possible deterioration of the water quality in the lagoon. The resulting average residence time for the entire lagoon with the new inlet is 26 % longer than the base scenario. The flushing time increased with over 80 % compared to the base scenario. The explanation for this high increase in flushing time could be the increase in average residence time of the northwestern part, from 6 to 18 days. It should be noted that the e-folding threshold is never actually reached in this scenario.

Building a new inlet and keeping Slusan open would lead to a improved water exchange in the lagoon. The results seem to indicate a decrease in average residence time with 22 % and a decreased flushing time by 33 % compared with the base scenario. But due to the lower flow velocities in Slusan, sedimentation issues are bound to worsen. Thus, this scenario offers the benefit of increased water quality at the cost of increased maintenance dredging in Slusan. How much more frequent the dredging should be is unknown.

It might be hard to gauge the ecological impact caused by closing Slusan and relying solely on the new inlet for the water exchange. It is also beyond the scope of this report to compare the economical benefits with possible ecological drawbacks. The same applies to the scenario with two inlets. It is difficult to judge if the increased dredging costs are justified by possibly improved conditions for wildlife in the lagoon. Further evaluations by relevant stakeholders could be conducted to address these questions.

There are a few potential sources of errors in the model. The DEM used to calculate model elevation is one of them. Especially given the fact that the original 5 x 5 m resolution had to be converted to a 10 x 10 m resolution due to limitations in computing power. This could have an impact on a wide range of different parameters in the model. For example, it could be the reason why some islands in the simulation seem to be easily flooded despite the said flooding not occurring in reality. Another example is the phenomena of tracking particles being pushed deep south into the lagoon and getting stuck, as shown in Figure 40a. The inability to model a 5 x 5 m grid is likely to limit the movement of particles. The processing and interpolation of all data also leaves ample room for error.

The complex geometry of FLS itself with many narrow channels and islands might also affect the performance of the model negatively, since it makes it hard to model the real shape of the

lagoon precisely. A 5 x 5 m mesh would have been better suited to reflect the actual state of the lagoon, as many of the canals are less wide than 10 m. But due to time constraints and lack of computational power, a 10 x 10 m mesh was used regardless.

Another likely source of uncertainty and error in the model is the bathymetry of the north-eastern part of the lagoon. Whilst the field expedition mapped large parts of the lagoon bathymetry, the heavy presence of birdlife in the northeast prevented further measurements.

One limitation with IPH-ECO is its inability to model sediment transport and sedimentation. The inlet near Slusan is highly dynamic area, with sedimentation occuring at a rapid pace due to the high sediment transport. This could have an effect on the water exchange in the lagoon system. This is yet another potential source of error pertaining the model.

The timing of the tracker particle release plays a role in influencing the residence time and flushing time. In all of the scenarios, the particles were released during a rise in sea water levels. This likely leads to a higher residence time. Should the particles instead have been released during a decrease in sea water levels, then a lower residence time would likely been the result.

The wet and dry algorithm within IPH seems to have an impact on the particle movement in the lagoon, thus affecting their residence time. As shown in Figure 53, the water extent is larger during high water levels.

If the sluice gates worked as intended in the model, then it would prevent the widespread flooding seen in Figure 53 when water levels reach over 0.5 m. The exaggerated widespread flooding could also possibly be linked to the workings of the modelling software itself.

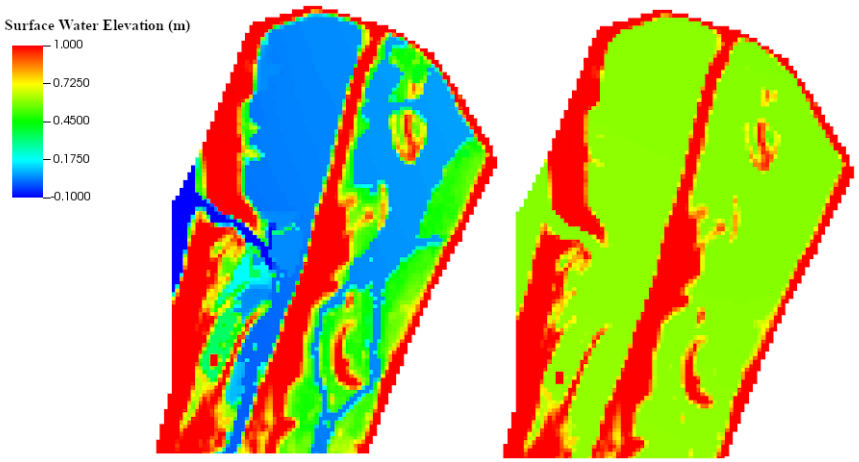

Figure 53: Images showing the effects of the wet and dry algorithm in the simulation results.

11 Conclusions and Recommendations

As stated in chapter 1.2, one of the objectives of this thesis was to determine the water exchange in the Flommen Lagoon system. To accomplish this, a working model capable of simulating the prevailing conditions in the lagoon had to be created. The creation of this model would also make possible the accomplishment of the second objective of this thesis, namely how to improve the water exchange in the lagoon, and hence the water quality. Both of these objectives were satisfactory achieved during the course of this thesis.

Whilst the created model is not a perfect carbon copy of reality, it was deemed reliable enough after the calibration and validation. This model was used to calculate the flushing time in different parts of the lagoon. As expected, given the narrow and elongated shape of the lagoon, residence time sees a general increase in the bodies of water further away from Slusan.

For the suggested improvements of the water exchange and water quality of Flommen, two simulation scenarios concerning the construction of a new inlet were considered. One of these simulated the effects on water exchange that two simultaneously open inlets would have on the lagoon. This simulation concluded that two open inlets would decrease the flushing time by 33 % compared with base scenario. Having two inlets open however, would decrease the flow velocities at Slusan, making sedimentation issues at Slusan worse. The other simulation simulated the lagoon with Slusan closed with the new inlet as its sole inlet. The results from this simulation indicated an increased of over 80 % in flushing time compared with the base scenario. The e-folding threshold is not reached during this scenario simulation.

If further studies are to be carried out on water exchange within the FLS, then a recommendation would be to conduct a field expedition to collect bathymetric data on the northeastern part of the lagoon. This would further enhance the accuracy of any future model.

Should a new inlet be desired to compliment Slusan, then it is suggested that additional investigation should be conducted regarding the expected increased sedimentation at Slusan.

12 Appendix

12.1 HOBO U20L Water Level Logger

The HOBO U20L records absolute pressure. As the logger is underwater, absolute pressure is in this case defined as atmospheric pressure plus the water head. If supplied with a starting reference water level, the accompanying HOBOware PRO software can convert the changes in absolute pressure to changes in water level. See Figure 54 for a picture of the logger.

Figure 54: Picture of a HOBO U20L Water Level Logger (Onset Computer Corporation, 2019).

12.2 HOBO Waterproof Shuttle U-DTW-1

The shuttle is vital for transferring data from a logger to a computer for further processing. It also acts as a medium between a logger and the computer, allowing the user to launch the logger recording immediately, or with a delay. See Figure 55 for a picture of the shuttle.

Figure 55: Picture of a HOBO Waterproof Shuttle U-DTW-1, with accompanying casings (Onset Computer Corporation, 2019).

12.3 Trimble SPS985 GNSS Smart Antenna

The Trimble SPS985 GNSS Smart Antenna was used to measure bathymetry in the Flommen Lagoon. Its water resistance and ease-of-use made it a reliable tool. See Figure 56 for a picture of the Trimble SPS985.

Figure 56: Picture of the Trimble SPS985 GNSS Smart Antenna (Trimble, 2020)

12.4 SWECO Measurements in Flommen

Figures 57 and 58 details salinity measurements made by SWECO.

Figure 57: Picture of different measurement points in SWECOs internal report about salinity in Flommen.

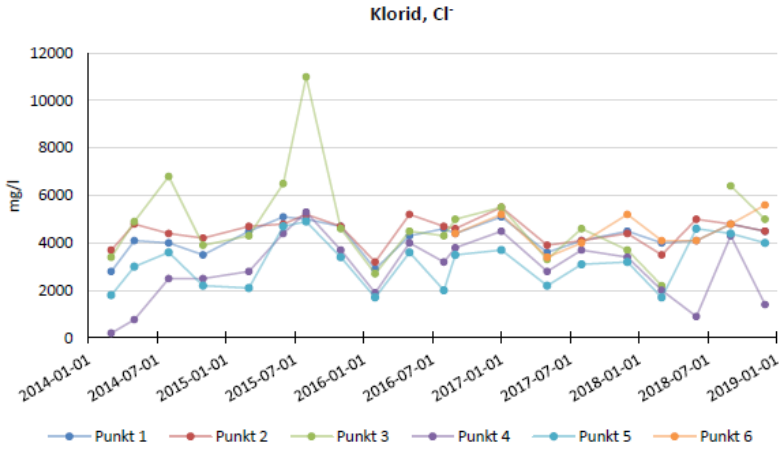

Figur 3 *Kloridhalter som uppmätts i de olika provtagningspunkterna under åren 2014–2018.*

Figure 58: Graph of different measurement points in SWECOs internal report about salinity in Flommen.

References

Barnes, R. (1980), *Coastal Lagoons*, Cambridge University Press.

Barnston, A. G. (1992), 'Correspondence among the correlation, RMSE, and heidke forecast verification measures; refinement of the heidke score', *Weather and Forecasting* **7**(4), 699–709.

Blomgren, S. (1999), *Hydrographic and Morphologic Processes at Falsterbo Peninsula: Present Conditions and Future Scenarios*, Department of Water Resources Engineering, Lund Institute of Technology, Lund University.

Danish Hydrological Institute (2018), 'Genomströmning flommens vattensystem: Desktop study for tidal inlet modifications at slusan', *Project Number 12804193* .

Davidson-Arnott, R. (2010), *Introduction to Coastal Processes and Geomorphology*, Cambridge University Press.

Davidsson, J. (1963), *Litoral Processes and Morphology on Scanian Flat-Coasts*, Meddelanden från Lunds universitets geografiska institution. Avhandlingar XLII., Gleerupska univ.-bokh.

de Brito Jr., A. N., Fragoso, Jr., C. R. and Larson, M. (2017), 'Tidal exchange in a choked coastal lagoon: A study of mundaú lagoon in northeastern brazil', *Regional Studies in Marine Science* **17**, 133–142.

Delhez, E., de Brye, B., de Brauwere, A. and Deleersnijder, E. (2014), 'Residence time vs influence time', *Journal of Marine Systems* **132**, 185–195.

Fragoso, Jr., C. R., van Nes, E. H., Janse, J. H. and da Motta Marques, D. (2009), 'Iphtrim3d-pclake: A three-dimensional complex dynamic model for subtropical aquatic ecosystems', *Elsevier* pp. 1347—-1348.

Hanson, H. (2007), 'Falsterbo peninsula, (sweden)', *Eurosion* .

Hanson, H. and Blomgren, S. (2000), 'Coastal geomorphology at the falsterbo peninsula, southern sweden', *Journal of Coastal Research* **16**(1), 15–25.

Hanson, H. and Larson, M. (1993), *'Sandtransport och kustutveckling vid Skanör/Falsterbo. (Swedish) [Sand Transport and Coastal Development at Skanör/Falsterbo]*, Department of Water Resources Engineering, Lund Institute of Technology, Lund University.

Hellström, B. (1941), *'Vattenståndsvariationerna i Östersjöbäckenet.' (Swedish) [Sea Level Variations in the Baltic Sea]*, Tekniskt Tidsskrift. Väg- och Vattenbyggnadskonst Husbyggnadsteknik.

Kjerfve, B. (1994), *Coastal Lagoon Processes*, Elsevier Science.

Kjerfve, B. and Magill, K. (1989), 'Geographic and hydrodynamic characteristics of shallow coastal lagoons', *Marine Geology* **88**, 187–199.

Kottek, M., Grieser, J., Beck, C., Rudolf, B. and Rubel, F. (2006), 'World map of the köppen-geiger climate classification updated', *Meteorologische Zeitschrift. (German) [Meteorological Journal]* **15**(3), 259–263.

Länsstyrelsen (2019), 'Flommen'. (Accessed 2020-02-28).
URL: *https://www.lansstyrelsen.se/skane/besoksmal/naturreservat/vellinge/flommen*

Manning, R. (1891), 'On the flow of water in open channels and pipes', *Transactions of the Institution of Civil Engineers of Ireland* **20**, 161—-207.

Miller, J. M., Pietrafesa, L. J. and Smith, N. P. (1990), *Principles of Hydraulic Management of Coastal Lagoons for Aquaculture and Fisheries.*

Nagelkerke, N. (1991), 'General circulation experiments with the primitive equations', *Biometrika* **78**(3), 691–692.

Pereira, F. F., Fragoso, Jr., C. R., Uvo, C. B., Collischonn, W. and da Motta Marques, D. (2013), 'Assessment of numerical schemes for solving the advection–diffusion equation on unstructured grids: case study of the guaíba river, brazil', *Nonlinear Processes in Geophysics* **20**, 1113–1125.

Rynne, P., Reniers, A., van de Kreeke, J. and MacMahan, J. (2016), 'The effect of tidal exchange on residence time in a coastal embayment', *Estuarine, Coastal and Shelf Science* **172**, 108–120.

Singh, V. P., Singh, P. and Haritashya, U. K. (2011), *Encyclopedia of Snow, Ice and Glaciers*, Springer, Dordrecht.

Smagorinsky, J. (1963), 'General circulation experiments with the primitive equations', *General Weather Review* **91**(3), 99—-164.

Swedish Meteorological and Hydrological Institute (2014), 'Sea level oscillations'. (Accessed 2020-02-26).
URL: *https://www.smhi.se/en/theme/sea-level-oscillations-1.12277*

Swedish Meteorological and Hydrological Institute (2019*a*), 'Open data for falsterbo, precipitation'. (Accessed 2020-02-26).
URL: *https://www.smhi.se/data/meteorologi/ladda-ner-meteorologiska-observationer/param=precipitationMonthlySum,stations=all*

Swedish Meteorological and Hydrological Institute (2019*b*), 'Open data for falsterbo, temperature'. (Accessed 2020-02-26).
URL: *https://www.smhi.se/data/meteorologi/ladda-ner-meteorologiska-observationer/param=airTemperatureMinAndMaxOnceEveryDay,stations=all*

Swedish Meteorological and Hydrological Institute (2020*a*), 'Meteorologiska observationer'. (Accessed 2020-02-26).
URL: *https://www.smhi.se/data/meteorologi/ladda-ner-meteorologiska-observationer/param=wind,stations=all,stationid=52230*

Swedish Meteorological and Hydrological Institute (2020*b*), 'Oceanografiska observationer'. (Accessed 2020-02-26).
URL: *https://www.smhi.se/data/oceanografi/ladda-ner-oceanografiska-observationer/param=sealevelrh2000,stations=all,stationid=30488*

US Army Corps of Engineers (1984), *Shore Protection Manual*, Dept. of the Army, Waterways Experiment Station, Corps of Engineers, Coastal Engineering Research Center.

Viero, D. P. and Defina, A. (2016), 'Water age, exposure time, and local flushing time in semi-enclosed, tidal basins with negligible freshwater inflow', *Journal of Marine Systems* **156**, 16–29.

Wang, S. (2019), *Modelling Water Exchange in the Flommen Lagoon, South Sweden*, Division of Water Resources Engineering, Department of Building and Environmental Technology, Lund University.